Spectral approximation of elliptic operators by the Hybrid High-Order method

Victor M Calo, Matteo Cicuttin, Quanling Deng, Alexandre Ern

Spectral approximation of elliptic operators by the Hybrid High-Order method

Victor Calo* Matteo Cicuttin† Quanling Deng‡ Alexandre Ern§

Abstract

We study the approximation of the spectrum of a second-order elliptic differential operator by the Hybrid High-Order (HHO) method. The HHO method is formulated using cell and face unknowns which are polynomials of some degree $k \geq 0$. Only cell unknowns correspond to eigenvalues and eigenfunctions, while the face unknowns help deliver superconvergence. Using the abstract theory of spectral approximation of compact operators in Hilbert spaces, we prove that the eigenvalues (super-)converge at rate $(2k+2)$ and the eigenfunctions at rate $(k+1)$ in the H^1-seminorm. Our theoretical findings are verified on various numerical examples including smooth and non-smooth eigenfunctions. Moreover, we observe numerically in one dimension a convergence rate of $(2k+4)$ for the eigenvalues for a specific value of the stabilization parameter. **Mathematics Subjects Classification**: 65N15, 65N30, 65N35, 35J05

Keywords Hybrid high-order methods, eigenvalue approximation, eigenfunction approximation, spectrum analysis, error analysis

1 Introduction

The Hybrid High-Order (HHO) method has been recently introduced for diffusion problems in [26] and for linear elasticity problems in [25]. The HHO method is formulated by introducing cell and face unknowns which are polynomials of some degree $k \geq 0$ (some variations in the degree of the cell unknowns are possible). The method is then devised from a local reconstruction operator and a (subtle) local stabilization operator in each mesh cell. This leads to a discretization method that supports general meshes (with

*Department of Applied Geology, Western Australian School of Mines, Curtin University, Kent Street, Bentley, Perth, WA 6102, Australia; Mineral Resources, Commonwealth Scientific and Industrial Research Organisation (CSIRO), Kensington, Perth, WA 6152, Australia. E-mail address: victor.calo@curtin.edu.au

†University Paris-Est, CERMICS (ENPC), 77455 Marne la Vallée cedex 2, and INRIA Paris, 75589 Paris, France. E-mail address: matteo.cicuttin@enpc.fr

‡Corresponding author. Curtin Institute for Computation and Department of Applied Geology, Western Australian School of Mines, Curtin University, Kent Street, Bentley, Perth, WA 6102, Australia. E-mail address: quanling.deng@curtin.edu.au

§University Paris-Est, CERMICS (ENPC), 77455 Marne la Vallée cedex 2, and INRIA Paris, 75589 Paris, France. E-mail address: alexandre.ern@enpc.fr

polyhedral cells and non-matching interfaces). Moreover, when approximating smooth solutions of the second-order elliptic source problems, the method delivers error estimates of order h^{k+1} in the H^1-seminorm and of order h^{k+2} in the L^2-norm under full elliptic regularity. Positioning unknowns at mesh faces is also a natural way to express locally in each mesh cell the balance properties satisfied by the model problem. As shown in [16], the HHO method can be fitted into the family of Hybridizable Discontinuous Galerkin (HDG) methods introduced in [17] and is also closely related to the nonconforming Virtual Element Method from [5] and the Weak Galerkin method from [44]. The HHO method has undergone a vigorous development over the last few years; we mention, among others, the application to advection-diffusion equations in [23], to the Stokes equations in [27], to the Leray–Lions equations in [22], and to hyperelasticity with finite deformations in [1]. The implementation of HHO methods is described in [15]. As already pointed out in [26, 25], the cell unknowns can be eliminated locally in each mesh cell, leading to a global Schur complement problem with compact stencil in terms of the face unknowns.

The goal of this work is to devise and analyze HHO methods for the discretization of the eigenvalue problem associated with a second-order elliptic differential operator. We formulate the discrete eigenvalue problem by letting the mass bilinear form act only on the cell unknowns, whereas the stiffness bilinear form acts, as for the discrete source problem, on both cell and face unknowns. For the error analysis on the discrete eigenvalues and eigenfunctions, we rely on the abstract theory of spectral approximation of compact operators in Hilbert spaces following the work of Vaĭnikko [42, 43], Bramble and Osborn [9, 38], Descloux et al. [20, 21], and Babuška and Osborn [6]. In this context, one key question is to identify the relevant HHO solution operator approximating the exact solution operator. We show that this can be achieved by introducing a purely cell-based HHO solution operator where the face unknowns have been eliminated by expressing them in terms of the cell unknowns. While this operator is not needed for actual computations, it plays a central role in the error analysis. The error analysis entails some further subtleties related to the special structure of the HHO reconstruction and stabilization operators. Our main result, see Theorem 4.4 and Corollary 4.6 below, establishes a convergence of order h^{2t} for the eigenvalues and of order h^t for the eigenfunctions in the H^1-seminorm where $t \in [s, k+1]$ is the smoothness index related to the eigenfunctions to be approximated and $s \in (\frac{1}{2}, 1]$ is the smoothness index resulting from the elliptic regularity theory. In the case of smooth eigenfunctions, we have $t = k+1$, leading to a convergence of order h^{2k+2} for the eigenvalues and of order h^{k+1} for the eigenfunctions in the H^1-seminorm. These superconvergence orders (polynomials of degree k are used) are confirmed by our numerical experiments including both smooth and non-smooth eigenfunctions of the Laplace operator in one and two dimensions. Finally, we mention that in one dimension, we observed an even better superconvergence of order h^{2k+4} for the eigenvalues whenever the stabilization parameter in the HHO method is chosen to be equal to $(2k+3)$.

Let us put our results in perspective with the literature on the approximation of elliptic eigenvalue problems by other discretization methods. Following the early work

in [41], it is well-known that using H^1-conforming finite elements of degree $k \geq 1$ on simplicial meshes leads to convergence rates of order h^{2k} for the eigenvalues and of order h^k for the eigenfunctions (provided the eigenfunctions are smooth enough). Similar results were obtained more recently in [3, 31] for discontinuous Galerkin (dG) methods. The analysis of the spectral approximation by mixed and mixed-hybrid methods was started in [13, 37, 36] and expanded in [29, 8]. Hybridization techniques leading to an eigenproblem on the face unknowns were studied in [18] for Raviart–Thomas mixed finite elements; therein, it was also observed that the use of a local post-processing technique improves the accuracy of the computed eigenfunctions (see also [30] for the lowest-order case). More recently, the spectral approximation of elliptic operators by the HDG method was analyzed in [32], leading to a convergence of order h^{2k+1} for the eigenvalues; therein, a non-trivial post-processing using a Rayleigh quotient was also examined numerically leading to an improved convergence of order h^{2k+2} for $k \geq 1$. In contrast, the HHO approximation directly delivers a provable convergence of order h^{2k+2} even for $k = 0$. Finally, let us mention the recent work in [39, 19, 12] which studies numerically the optimally blended quadrature rules [2] for the isogeometric analysis [34] of the Laplace eigenvalue problem and reports superconvergence of order h^{2k+2} for the eigenvalue errors while maintaining optimal convergence of orders h^k and h^{k+1} for the eigenfunction errors in the H^1-seminorm and in the L^2-norm, respectively.

The rest of this paper is organized as follows. Section 2 presents the second-order elliptic eigenvalue problem and briefly recalls the main abstract results we are going to use concerning the spectral approximation of compact operators in Hilbert spaces. Section 3 deals with the HHO discretization, first of the source problem and then of the eigenvalue problem. The algebraic realization of both problems is also presented. Section 3 additionally identifies the relevant notion of discrete solution operator for HHO methods and outlines the error analysis for the HHO discretization of the source problem. This analysis is based on the results of [26]; one novelty here is that we handle the case where the exact solution may not have full regularity to deliver optimally convergent error estimates. Section 4 is concerned with the error analysis for the HHO discretization of the eigenvalue problem and contains our main results. Section 5 presents our numerical examples. Finally, some concluding remarks are collected in Section 6.

2 Functional setting

In this section, we present the second-order elliptic eigenvalue problem, and briefly recall the main abstract results on the approximation of the spectrum of compact operators in Hilbert spaces.

2.1 Problem statement

We consider the following second-order elliptic eigenvalue problem: Find an eigenpair (λ, u) with $\lambda \in \mathbb{R}_{>0}$ and $u : \Omega \to \mathbb{R}$ such that

$$\begin{aligned} -\Delta u &= \lambda u \quad \text{in } \Omega, \\ u &= 0 \quad \text{on } \partial\Omega, \end{aligned} \tag{2.1}$$

where $\Omega \subset \mathbb{R}^d$, $d \in \{1, 2, 3\}$, is a bounded open domain with Lipschitz boundary $\partial\Omega$ and Δ is the Laplacian. In weak form, the problem (2.1) reads as follows: Find $(\lambda, u) \in \mathbb{R}_{>0} \times H_0^1(\Omega)$ such that

$$a(u, w) = \lambda b(u, w), \qquad \forall w \in H_0^1(\Omega), \tag{2.2}$$

with the bilinear forms a and b defined on $H_0^1(\Omega) \times H_0^1(\Omega)$ and $L^2(\Omega) \times L^2(\Omega)$ as

$$a(v, w) = (\nabla v, \nabla w)_{L^2(\Omega)}, \qquad b(v, w) = (v, w)_{L^2(\Omega)}, \tag{2.3}$$

where $(\cdot, \cdot)_{L^2(\Omega)}$ denotes the inner product in $L^2(\Omega)$ or in $L^2(\Omega; \mathbb{R}^d)$. The eigenvalue problem (2.1) has a countably infinite sequence of eigenvalues $(\lambda_j)_{j \geq 1}$ (see, among many others, [11, Sec. 9.8]) such that

$$0 < \lambda_1 < \lambda_2 \leq \lambda_3 \leq \cdots, \qquad \lambda_j \to +\infty, \tag{2.4}$$

and an associated sequence of L^2-orthonormal eigenfunctions $(u_j)_{j \geq 1}$ such that

$$(u_j, u_k)_{L^2(\Omega)} = \delta_{jk}, \qquad \forall j, k \geq 1, \tag{2.5}$$

with the Kronecker delta defined as $\delta_{jk} = 1$ when $j = k$ and zero otherwise.

The source problem associated with the eigenvalue problem (2.2) is as follows: For all $\phi \in L^2(\Omega)$, find $u \in H_0^1(\Omega)$ such that

$$a(u, w) = b(\phi, w), \qquad \forall w \in H_0^1(\Omega). \tag{2.6}$$

The solution operator associated with (2.6) is denoted as $T : L^2(\Omega) \to L^2(\Omega)$, so that we have $T(\phi) \in H_0^1(\Omega) \subset L^2(\Omega)$ and

$$a(T(\phi), w) = b(\phi, w), \qquad \forall w \in H_0^1(\Omega). \tag{2.7}$$

By the Rellich–Kondrachov Theorem (see, e.g., [33, Thm. 1.4.3.2]), T is compact from $L^2(\Omega)$ to $L^2(\Omega)$. Moreover, the elliptic regularity theory (see, e.g., [33, 40, 35]) implies that there is a real number $s \in (\frac{1}{2}, 1]$ so that $T \in \mathcal{L}(L^2(\Omega); H^{1+s}(\Omega))$. The reason for introducing the solution operator T is that $(\lambda, u) \in \mathbb{R}_{>0} \times H_0^1(\Omega)$ is an eigenpair for (2.2) if and only if $(\mu, u) \in \mathbb{R}_{>0} \times H_0^1(\Omega)$ with $\mu = \lambda^{-1}$ is an eigenpair of T.

One can also consider the adjoint solution operator $T^* : L^2(\Omega) \to L^2(\Omega)$ such that, for all $\psi \in L^2(\Omega)$, $T^*(\psi) \in H_0^1(\Omega)$ and

$$a(w, T^*(\psi)) = b(w, \psi), \qquad \forall w \in H_0^1(\Omega). \tag{2.8}$$

The symmetry of the bilinear forms a and b implies that $T = T^*$; however, allowing more generality, we keep a distinct notation for the two operators. Since in general we have

$$(T(\phi),\psi)_{L^2(\Omega)} = a(T(\phi),T^*(\psi)) = (\phi,T^*(\psi))_{L^2(\Omega)}, \tag{2.9}$$

we infer that T^* is the adjoint operator of T, once the duality product is identified with the inner product in $L^2(\Omega)$. Therefore, in the present symmetric context, the operator T is selfadjoint.

2.2 Spectral approximation theory for compact operators

Let us now briefly recall the main results we use concerning the spectral approximation of compact operators in Hilbert spaces. Let L be a Hilbert space with inner product denoted by $(\cdot,\cdot)_L$, and let $T \in \mathcal{L}(L;L)$; assume that T is compact. We do not assume for the abstract theory that T is selfadjoint and we let $T^* \in \mathcal{L}(L;L)$ denote the adjoint operator of T. Let $T_n \in \mathcal{L}(L;L)$ be a member of a sequence of compact operators that converges to T in operator norm, i.e.,

$$\lim_{n\to+\infty} \|T - T_n\|_{\mathcal{L}(L;L)} = 0, \tag{2.10}$$

and let $T_n^* \in \mathcal{L}(L;L)$ be the adjoint operator of T_n. We want to study how well the eigenvalues and the eigenfunctions of T_n approximate those of T. Let $\sigma(T)$ denote the spectrum of the operator T and let $\mu \in \sigma(T) \setminus \{0\}$ be a nonzero eigenvalue of T. Let α be the ascent of μ, i.e., the smallest integer α such that $\ker(\mu I - T)^\alpha = \ker(\mu I - T)^{\alpha+1}$, where I is the identity operator. Let also

$$G_\mu = \ker(\mu I - T)^\alpha, \qquad G_\mu^* = \ker(\mu I - T^*)^\alpha, \tag{2.11}$$

and $m = \dim(G_\mu)$ (this integer is called the algebraic multiplicity of μ; note that $m \geq \alpha$).

Theorem 2.1 (Convergence of the eigenvalues)**.** *Let $\mu \in \sigma(T) \setminus \{0\}$. Let α be the ascent of μ and let m be its algebraic multiplicity. Then there are m eigenvalues of T_n, denoted as $\mu_{n,1},\cdots,\mu_{n,m}$, that converge to μ as $n \to +\infty$. Moreover, letting $\langle\mu_n\rangle = \frac{1}{m}\sum_{j=1}^m \mu_{n,j}$ denote their arithmetic mean, there is C, depending on μ but independent of n, such that*

$$\begin{aligned}\max_{1\leq j\leq m} |\mu - \mu_{n,j}|^\alpha + |\mu - \langle\mu_n\rangle| \leq C\Big(&\sup_{\substack{0\neq\phi\in G_\mu\\ 0\neq\psi\in G_\mu^*}} \frac{|((T-T_n)\phi,\psi)_L|}{\|\phi\|_L\|\psi\|_L} \\ &+ \|(T-T_n)|_{G_\mu}\|_{\mathcal{L}(G_\mu;L)}\|(T-T_n)^*|_{G_\mu^*}\|_{\mathcal{L}(G_\mu^*;L)}\Big).\end{aligned} \tag{2.12}$$

Remark 2.2 (Convergence of the arithmetic mean)**.** Note that (2.12) shows that for $\alpha \geq 2$, the arithmetic mean of the eigenvalues has a better convergence rate than each eigenvalue individually.

Theorem 2.3 (Convergence of the eigenfunctions)**.** *Let $\mu \in \sigma(T) \setminus \{0\}$ with ascent α and algebraic multiplicity μ. Let $\mu_{n,j}$ be an eigenvalue of T_n that converges to μ. Let $w_{n,j}$ be a unit vector in $ker(\mu_{n,j}I - T_n)^\ell$ for some positive integer $\ell \le \alpha$. Then, for any integer m with $\ell \le m \le \alpha$, there is a vector $u_m \in \ker(\mu I - T)^m \subset G_\mu$ such that*

$$\|u_m - w_{n,j}\|_L \le C\|(T - T_n)|_{G_\mu}\|^{\frac{m-\ell+1}{\alpha}}_{\mathcal{L}(G_\mu;L)}, \tag{2.13}$$

where C depends on μ but is independent of n.

3 HHO discretization

In this section we present the discrete setting underlying the HHO discretization and then describe the discretization of the source problem (2.6) and of the eigenvalue problem (2.2) by the HHO method. The HHO discretization of the source problem has been introduced and analyzed in [26]; herein, we complete the error analysis by addressing the case where the solution has minimal elliptic regularity pickup. The devising and analysis of the HHO discretization of the eigenvalue problem is the main subject of this work.

3.1 Discrete setting

Let $\mathcal{K}$ be a partition of Ω into non-overlapping mesh cells. A generic mesh cell is denoted by K and can be a d-dimensional polytope with planar faces. In what follows, we assume that Ω is also a polytope in $\mathbb{R}^d$ with planar faces, so that the mesh can cover Ω exactly. For all $K \in \mathcal{K}$, we let $\boldsymbol{n}_K$ denote the unit outward vector to K. We say that $F \subset \mathbb{R}^d$ is a mesh face if it is a subset with nonempty relative interior of some affine hyperplane H_F. If there are two distinct mesh cells $K_1, K_2 \in \mathcal{K}$ so that $F = \partial K_1 \cap \partial K_2 \cap H_F$, then F is called an interface. Alternatively, if there is one mesh cell $K \in \mathcal{K}$ so that $F = \partial K \cap \partial\Omega \cap H_F$, then F is called a boundary face. The mesh faces are collected in the set $\mathcal{F}$, interfaces in the set $\mathcal{F}^{\mathrm{i}}$, and boundary faces in the set $\mathcal{F}^{\mathrm{b}}$. We let h_S denote the diameter of the set S which can be a mesh cell or a mesh face. We assume that the mesh $\mathcal{K}$ is a member of a shape-regular polytopal mesh family in the sense specified in [26, 25]. In a nutshell, there is a matching simplicial submesh of $\mathcal{K}$ that belongs to a shape-regular family of simplicial meshes in the usual sense of Ciarlet [14] and such that each cell $K \in \mathcal{K}$ (resp., face $F \in \mathcal{F}$) can be decomposed in a finite number of sub-cells (resp., sub-faces) with uniformly comparable diameter.

The HHO method is defined locally in each mesh cell $K \in \mathcal{K}$ from a pair of local unknowns which consist of one polynomial attached to the cell K and a piecewise polynomial attached to the boundary ∂K, i.e., one polynomial attached to each face F composing the boundary of K. Let $k \ge 0$ be a polynomial degree, and let $\mathbb{P}^k_{d'}(S)$, with $d' \in \{d-1, d\}$ be the linear space composed of real-valued polynomials of total degree at most k on the d'-dimensional affine manifold $S \subset \mathbb{R}^d$ (S is typically a mesh face or a mesh cell). The local discrete HHO pair is denoted

$$\hat{v}_K = (v_K, v_{\partial K}) \in \hat{V}_K^k := \mathbb{P}^k_d(K) \times \mathbb{P}^k_{d-1}(\mathcal{F}_{\partial K}), \tag{3.1}$$

where

$$\mathbb{P}^k_{d-1}(\mathcal{F}_{\partial K}) = \bigtimes_{F\in\mathcal{F}_{\partial K}} \mathbb{P}^k_{d-1}(F), \tag{3.2}$$

and $\mathcal{F}_{\partial K}$ is the collection of all the faces composing the cell boundary ∂K. There is actually some flexibility in the choice of the polynomial degree for the cell unknowns since one can take them to be polynomials of degree $l \in \{k-1, k, k+1\}$ [16]. For simplicity, we only consider the case $l = k$; all what follows readily extends to the other choices for l. In what follows, we always use hat symbols to indicate discrete HHO pairs.

There are two key ingredients to devise locally the HHO method: a local reconstruction operator and a local stabilization operator. The local reconstruction operator is defined as $p^{k+1}_K : \hat{V}^k_K \to \mathbb{P}^{k+1}_d(K)$ such that for all $\hat{v}_K = (v_K, v_{\partial K}) \in \hat{V}^k_K$, we have

$$(\nabla p^{k+1}_K(\hat{v}_K), \nabla w)_{L^2(K)} = (\nabla v_K, \nabla w)_{L^2(K)} + (v_{\partial K} - v_K, \nabla w\cdot\boldsymbol{n}_K)_{L^2(\partial K)}, \tag{3.3}$$

for all $w \in \mathbb{P}^{k+1}_d(K)$. The above Neumann problem uniquely defines $p^{k+1}_K(\hat{v}_K) \in \mathbb{P}^{k+1}_d(K)$ up to an additive constant which can be specified by additionally requiring that $(p^{k+1}_K(\hat{v}_K) - v_K, 1)_{L^2(K)} = 0$ (this choice is irrelevant in what follows). Concerning stabilization, we define the local operator $S^k_{\partial K} : \hat{V}^k_K \to \mathbb{P}^k_{d-1}(\mathcal{F}_{\partial K})$ such that, for all $\hat{v}_K = (v_K, v_{\partial K}) \in \hat{V}^k_K$, we have

$$S^k_{\partial K}(\hat{v}_K) = \Pi^k_{\partial K}(v_{\partial K} - \gamma_{\partial K}(p^{k+1}_K(\hat{v}_K))) - \gamma_{\partial K}(\Pi^k_K(v_K - p^{k+1}_K(\hat{v}_K))), \tag{3.4}$$

where $\gamma_{\partial K}$ denotes the trace map, i.e., the restriction to the boundary ∂K and Π^k_K and $\Pi^k_{\partial K}$ denote the L^2-orthogonal projectors from $L^1(K)$ onto $\mathbb{P}^k_d(K)$ and from $L^1(\partial K)$ onto $\mathbb{P}^k_{d-1}(\mathcal{F}_{\partial K})$, respectively. By slightly abusing the notation and letting $\Pi^k_{\partial K}$ act also on functions defined on K with the understanding that the trace is actually considered, we can write $S^k_{\partial K}(\hat{v}_K) = \Pi^k_{\partial K}(v_{\partial K} - P^{k+1}_K(\hat{v}_K))$ with $P^k_K(\hat{v}_K) = v_K + (I - \Pi^k_K)(p^k_K(\hat{v}_K))$, which is [26, Eq. (22)]. Finally, the local HHO bilinear form for the stiffness is such that, for all $\hat{v}_K = (v_K, v_{\partial K}) \in \hat{V}^k_K$ and all $\hat{w}_K = (w_K, w_{\partial K}) \in \hat{V}^k_K$, we have

$$\hat{a}_K(\hat{v}_K, \hat{w}_K) = (\nabla p^{k+1}_K(\hat{v}_K), \nabla p^{k+1}_K(\hat{w}_K))_{L^2(K)} + (\tau_{\partial K} S^k_{\partial K}(\hat{v}_K), S^k_{\partial K}(\hat{w}_K))_{L^2(\partial K)}, \tag{3.5}$$

where $\tau_{\partial K}$ denotes the piecewise constant function on ∂K such that $\tau_{\partial K|F} = \eta h_F^{-1}$ for all $F \in \mathcal{F}_{\partial K}$, and $\eta > 0$ is a user-specified positive stabilization parameter (the simplest choice is to set $\eta = 1$).

3.2 HHO discretization of the source problem

Let $\phi \in L^2(\Omega)$. To discretize the source problem (2.6) using the HHO method, we consider the following global space of discrete HHO pairs:

$$\hat{V}^k_h = V^k_{\mathcal{K}} \times V^k_{\mathcal{F}}, \qquad V^k_{\mathcal{K}} = \bigtimes_{K\in\mathcal{K}} \mathbb{P}^k_d(K), \qquad V^k_{\mathcal{F}} = \bigtimes_{F\in\mathcal{F}} \mathbb{P}^k_{d-1}(F). \tag{3.6}$$

Here, the subscript h refers to the global mesh-size defined as $h = \max_{K\in\mathcal{K}} h_K$. For a global HHO pair $\hat{v}_h = (v_{\mathcal{K}}, v_{\mathcal{F}}) \in \hat{V}^k_h$ with $v_{\mathcal{K}} \in V^k_{\mathcal{K}}$ and $v_{\mathcal{F}} \in V^k_{\mathcal{F}}$, we denote by $\hat{v}_K =$

$(v_K, v_{\partial K}) \in \hat{V}_K^k$ the local HHO pair associated with the mesh cell $K \in \mathcal{K}$, and we denote by $v_F \in \mathbb{P}_{d-1}^k(F)$ the component associated with the mesh face $F \in \mathcal{F}$. The homogeneous Dirichlet boundary condition can be embedded into the HHO space by considering the subspaces

$$\hat{V}_{h,0}^k := V_{\mathcal{K}}^k \times V_{\mathcal{F},0}^k, \qquad V_{\mathcal{F},0}^k := \{v_{\mathcal{F}} \in V_{\mathcal{F}}^k \mid v_F = 0, \ \forall F \in \mathcal{F}^{\mathrm{b}}\}. \tag{3.7}$$

The HHO discretization of the source problem reads as follows: Find $\hat{u}_h \in \hat{V}_{h,0}^k$ such that

$$\hat{a}_h(\hat{u}_h, \hat{w}_h) = b(\phi, w_{\mathcal{K}}), \qquad \forall \hat{w}_h = (w_{\mathcal{K}}, w_{\mathcal{F}}) \in \hat{V}_{h,0}^k, \tag{3.8}$$

where, for all $\hat{v}_h, \hat{w}_h \in \hat{V}_h$, we have set

$$\hat{a}_h(\hat{v}_h, \hat{w}_h) = \sum_{K \in \mathcal{K}} \hat{a}_K(\hat{v}_K, \hat{w}_K). \tag{3.9}$$

The algebraic realization of the discrete source problem (3.8) leads to a symmetric positive-definite linear system which can be written in the following block form where unknowns attached to mesh cells are ordered before unknowns attached to mesh faces:

$$\begin{bmatrix} \mathbf{A}_{\mathcal{K}\mathcal{K}} & \mathbf{A}_{\mathcal{K}\mathcal{F}} \\ \mathbf{A}_{\mathcal{F}\mathcal{K}} & \mathbf{A}_{\mathcal{F}\mathcal{F}} \end{bmatrix} \begin{bmatrix} \mathbf{U}_{\mathcal{K}} \\ \mathbf{U}_{\mathcal{F}} \end{bmatrix} = \begin{bmatrix} \boldsymbol{\phi}_{\mathcal{K}} \\ \mathbf{0} \end{bmatrix}. \tag{3.10}$$

A computationally-effective way to solve this linear system is to use a Schur complement technique (also known as static condensation) where the cell unknowns are eliminated by expressing them locally in terms of the face unknowns. This elimination is simple since the submatrix $\mathbf{A}_{\mathcal{K}\mathcal{K}}$ is block-diagonal. The resulting linear system in terms of the face unknowns is

$$\mathbf{K}_{\mathcal{F}\mathcal{F}}\mathbf{U}_{\mathcal{F}} = -\mathbf{A}_{\mathcal{F}\mathcal{K}}\mathbf{A}_{\mathcal{K}\mathcal{K}}^{-1}\boldsymbol{\phi}_{\mathcal{K}}, \tag{3.11}$$

with the Schur complement matrix $\mathbf{K}_{\mathcal{F}\mathcal{F}} = \mathbf{A}_{\mathcal{F}\mathcal{F}} - \mathbf{A}_{\mathcal{F}\mathcal{K}}\mathbf{A}_{\mathcal{K}\mathcal{K}}^{-1}\mathbf{A}_{\mathcal{K}\mathcal{F}}$. As shown in [16], the linear system (3.11) is a global transmission problem (in which a given mesh face is locally coupled to the other mesh faces with which it shares a mesh cell) that expresses the equilibration of a suitable flux across all the mesh interfaces.

3.3 HHO discretization of the eigenvalue problem

The HHO discretization of the eigenvalue problem (2.2) consists of finding the discrete eigenpairs $(\lambda_h, \hat{u}_h) \in \mathbb{R}_{>0} \times \hat{V}_{h,0}^k$ such that

$$\hat{a}_h(\hat{u}_h, \hat{w}_h) = \lambda_h b(u_{\mathcal{K}}, w_{\mathcal{K}}), \qquad \forall \hat{w}_h = (w_{\mathcal{K}}, w_{\mathcal{F}}) \in \hat{V}_{h,0}^k. \tag{3.12}$$

The mass bilinear form on the right-hand side of (3.12) only involves discrete cell unknowns.

The algebraic realization of (3.12) is the matrix eigenvalue problem

$$\begin{bmatrix} \mathbf{A}_{\mathcal{K}\mathcal{K}} & \mathbf{A}_{\mathcal{K}\mathcal{F}} \\ \mathbf{A}_{\mathcal{F}\mathcal{K}} & \mathbf{A}_{\mathcal{F}\mathcal{F}} \end{bmatrix} \begin{bmatrix} \mathbf{U}_{\mathcal{K}} \\ \mathbf{U}_{\mathcal{F}} \end{bmatrix} = \lambda_h \begin{bmatrix} \mathbf{B}_{\mathcal{K}\mathcal{K}} & \mathbf{0} \\ \mathbf{0} & \mathbf{0} \end{bmatrix} \begin{bmatrix} \mathbf{U}_{\mathcal{K}} \\ \mathbf{U}_{\mathcal{F}} \end{bmatrix}. \tag{3.13}$$

Since the face unknowns do not carry any mass, they can be eliminated, leading to the following matrix eigenvalue problem solely in terms of the cell unknowns:

$$\mathbf{K}_{\mathcal{K}\mathcal{K}}\mathbf{U}_{\mathcal{K}} = \lambda_h \mathbf{B}_{\mathcal{K}\mathcal{K}}\mathbf{U}_{\mathcal{K}}, \tag{3.14}$$

with the Schur complement matrix $\mathbf{K}_{\mathcal{K}\mathcal{K}} = \mathbf{A}_{\mathcal{K}\mathcal{K}} - \mathbf{A}_{\mathcal{K}\mathcal{F}}\mathbf{A}_{\mathcal{F}\mathcal{F}}^{-1}\mathbf{A}_{\mathcal{F}\mathcal{K}}$. Therefore, there are as many discrete eigenpairs as there are cell unknowns, i.e., the dimension of the space $V_{\mathcal{K}}^k$ which is equal to the dimension of the polynomial space $\mathbb{P}_d^k$ times the number of mesh cells.

3.4 HHO solution operators

Consider the HHO discretization of the source problem (3.8). We can define the cell-face HHO solution operator $\hat{T}_h : L^2(\Omega) \to \hat{V}_{h,0}^k$ so that

$$\hat{a}_h(\hat{T}_h(\phi), \hat{w}_h) = b(\phi, w_{\mathcal{K}}), \qquad \forall \hat{w}_h = (w_{\mathcal{K}}, w_{\mathcal{F}}) \in \hat{V}_{h,0}^k. \tag{3.15}$$

However, the operator $\hat{T}_h$ is not convenient to handle since it does not map to a subspace of $L^2(\Omega)$. The key idea is then to introduce a cell HHO solution operator $T_{\mathcal{K}} : L^2(\Omega) \to V_{\mathcal{K}}^k \subset L^2(\Omega)$ by mimicking the elimination of the face unknowns presented above at the algebraic level for the eigenvalue problem.

As a first step, we define the operator $Z_{\mathcal{F},0} : V_{\mathcal{K}}^k \to V_{\mathcal{F},0}^k$ so that, for all $v_{\mathcal{K}} \in V_{\mathcal{K}}^k$, $Z_{\mathcal{F},0}(v_{\mathcal{K}}) \in V_{\mathcal{F},0}^k$ is defined as the unique solution of

$$\hat{a}_h((v_{\mathcal{K}}, Z_{\mathcal{F},0}(v_{\mathcal{K}})), (0, w_{\mathcal{F}})) = 0, \qquad \forall w_{\mathcal{F}} \in V_{\mathcal{F},0}^k. \tag{3.16}$$

To allow for some generality, we also define the operator $Z_{\mathcal{F},0}^\dagger : V_{\mathcal{K}}^k \to V_{\mathcal{F},0}^k$ so that

$$\hat{a}_h((0, w_{\mathcal{F}}), (v_{\mathcal{K}}, Z_{\mathcal{F},0}^\dagger(v_{\mathcal{K}}))) = 0, \qquad \forall w_{\mathcal{F}} \in V_{\mathcal{F},0}^k. \tag{3.17}$$

In the present setting where the bilinear form $\hat{a}_h$ is symmetric, the two operators $Z_{\mathcal{F},0}$ and $Z_{\mathcal{F},0}^\dagger$ coincide. As a second step, we define the bilinear form $a_{\mathcal{K}}$ on $V_{\mathcal{K}}^k \times V_{\mathcal{K}}^k$ such that

$$a_{\mathcal{K}}(v_{\mathcal{K}}, w_{\mathcal{K}}) = \hat{a}_h((v_{\mathcal{K}}, Z_{\mathcal{F},0}(v_{\mathcal{K}})), (w_{\mathcal{K}}, Z_{\mathcal{F},0}^\dagger(w_{\mathcal{K}}))), \tag{3.18}$$

and introduce the solution operator $T_{\mathcal{K}} : L^2(\Omega) \to V_{\mathcal{K}}^k$ so that

$$a_{\mathcal{K}}(T_{\mathcal{K}}(\phi), w_{\mathcal{K}}) = b(\phi, w_K), \qquad \forall w_{\mathcal{K}} \in V_{\mathcal{K}}^k. \tag{3.19}$$

Lemma 3.1 (HHO solution operator)**.** *The following holds:*

$$\hat{T}_h(\phi) = (T_{\mathcal{K}}(\phi), (Z_{\mathcal{F},0} \circ T_{\mathcal{K}})(\phi)), \qquad \forall \phi \in L^2(\Omega). \tag{3.20}$$

Proof. Let $\phi \in L^2(\Omega)$. Let us set $u_{\mathcal{K}} = T_{\mathcal{K}}(\phi)$ so that $u_{\mathcal{K}} \in V_{\mathcal{K}}^k$ and $a_{\mathcal{K}}(u_{\mathcal{K}}, w_{\mathcal{K}}) = b(\phi, w_{\mathcal{K}})$, for all $w_{\mathcal{K}} \in V_{\mathcal{K}}^k$. Let us set $u_{\mathcal{F}} = (Z_{\mathcal{F},0} \circ T_{\mathcal{K}})(\phi) = Z_{\mathcal{F},0}(u_{\mathcal{K}})$ so that $u_{\mathcal{F}} \in V_{\mathcal{F},0}^k$. Setting

$\hat{u}_h = (u_{\mathcal{K}}, u_{\mathcal{F}}) \in \hat{V}_{h,0}^k$, we need to verify that $\hat{u}_h$ solves the discrete HHO source problem, i.e.,

$$\hat{a}_h(\hat{u}_h, \hat{w}_h) = b(\phi, w_{\mathcal{K}}), \qquad \forall \hat{w}_h = (w_{\mathcal{K}}, w_{\mathcal{F}}) \in \hat{V}_{h,0}^k.$$

Considering first a test function in the form $\hat{w}_h = (w_{\mathcal{K}}, 0)$, we obtain

$$\begin{aligned}
\hat{a}_h(\hat{u}_h, (w_{\mathcal{K}}, 0)) &= \hat{a}_h((u_{\mathcal{K}}, Z_{\mathcal{F},0}(u_{\mathcal{K}})), (w_{\mathcal{K}}, 0)) \\
&= \hat{a}_h((u_{\mathcal{K}}, Z_{\mathcal{F},0}(u_{\mathcal{K}})), (w_{\mathcal{K}}, 0)) + \underbrace{\hat{a}_h((u_{\mathcal{K}}, Z_{\mathcal{F},0}(u_{\mathcal{K}})), (0, Z_{\mathcal{F},0}^{\dagger}(w_{\mathcal{K}})))}_{=0} \\
&= \hat{a}_h((u_{\mathcal{K}}, Z_{\mathcal{F},0}(u_{\mathcal{K}})), (w_{\mathcal{K}}, Z_{\mathcal{F},0}^{\dagger}(w_{\mathcal{K}}))) \\
&= a_{\mathcal{K}}(u_{\mathcal{K}}, w_{\mathcal{K}}) = b(\phi, w_{\mathcal{K}}),
\end{aligned}$$

where we use the definition (3.16) of $Z_{\mathcal{F},0}$ in the second line and the definition (3.18) of $a_{\mathcal{K}}$ in the fourth line. Considering now a test function in the form $\hat{w}_h = (0, w_{\mathcal{F}})$, we obtain owing to (3.16) that

$$\hat{a}_h(\hat{u}_h, (0, w_{\mathcal{F}})) = \hat{a}_h((u_{\mathcal{K}}, Z_{\mathcal{F},0}(u_{\mathcal{K}})), (0, w_{\mathcal{F}})) = 0.$$

This completes the proof. □

The cell HHO solution operator $T_{\mathcal{K}}$ defined in (3.19) is the relevant solution operator for the discrete eigenvalue problem (3.12). Indeed, the eigenpair $(\lambda_h, \hat{u}_h) \in \mathbb{R}_{>0} \times \hat{V}_{h,0}^k$ with $\hat{u}_h = (u_{\mathcal{K}}, u_{\mathcal{F}}) \in V_{\mathcal{K}}^k \times V_{\mathcal{F},0}^k$ solves (3.12) if and only if $u_{\mathcal{F}} = Z_{\mathcal{F},0}(u_{\mathcal{K}})$ and the pair $(\lambda_h, u_{\mathcal{K}}) \in \mathbb{R}_{>0} \times V_{\mathcal{K}}^k$ solves

$$a_{\mathcal{K}}(u_{\mathcal{K}}, w_{\mathcal{K}}) = \lambda_h b(u_{\mathcal{K}}, w_{\mathcal{K}}), \qquad \forall w_{\mathcal{K}} \in V_{\mathcal{K}}^k, \tag{3.21}$$

that is, if and only if $(\mu_h, u_{\mathcal{K}}) \in \mathbb{R}_{>0} \times V_{\mathcal{K}}^k$ with $\mu_h = \lambda_h^{-1}$ is an eigenpair of the discrete solution operator $T_{\mathcal{K}}$.

3.5 Error analysis for the source problem

In this section we briefly outline the analysis of the HHO discretization of the source problem drawing on the ideas introduced in [26]. One novelty here is to include the case when the exact solution has a smoothness index $s \in (\frac{1}{2}, k+2]$ and not just $s = k+2$ (recall that $s > \frac{1}{2}$ follows from the elliptic regularity theory). In what follows, we use the symbol C to denote a generic constant (its value can change at each occurrence) that can depend on the mesh regularity, the polynomial degree k and the domain Ω, but is independent of the mesh-size h.

Let $K \in \mathcal{K}$ be a mesh cell. We equip the local HHO space $\hat{V}_K^k$ defined in (3.1) with the following seminorm (which is an HHO counterpart of the $H^1(K)$-seminorm)

$$\|\hat{v}_K\|_{\hat{a}_K}^2 = \|\nabla v_K\|_{L^2(K)}^2 + \|\tau_{\partial K}^{\frac{1}{2}}(v_K - v_{\partial K})\|_{L^2(\partial K)}^2, \tag{3.22}$$

for all $\hat{v}_K = (v_K, v_{\partial K}) \in \hat{V}_K^k$. We observe that $\|\hat{v}_K\|_{\hat{V}_K^k} = 0$ implies that v_K and $v_{\partial K}$ are constant functions taking the same value. We equip the global HHO space $\hat{V}_h^k$ defined in (3.6) with the seminorm (which is an HHO counterpart of the $H^1(\Omega)$-seminorm)

$$\|\hat{v}_h\|_{\hat{a}_h}^2 = \sum_{K\in\mathcal{K}} \|\hat{v}_K\|_{\hat{a}_K}^2, \qquad \forall \hat{v}_h \in \hat{V}_h^k. \tag{3.23}$$

The map $\|\cdot\|_{\hat{a}_h}$ is a norm on the subspace $\hat{V}_{h,0}^k$ defined in (3.7). [26, Lemma 4] shows that there is a real number $\beta > 0$, uniform with respect to the mesh-size h, such that, for all $K \in \mathcal{K}$,

$$\beta\|\hat{v}_K\|_{\hat{a}_K}^2 \le \hat{a}_K(\hat{v}_K, \hat{v}_K) \le \beta^{-1}\|\hat{v}_K\|_{\hat{a}_K}^2, \qquad \forall \hat{v}_K \in \hat{V}_K^k, \tag{3.24}$$

and, consequently, given the definition (3.9) of $\hat{a}_h$, that the following coercivity and boundedness properties hold true:

$$\hat{a}_h(\hat{v}_h, \hat{v}_h) \ge \beta\|\hat{v}_h\|_{\hat{a}_h}^2, \qquad \forall \hat{v}_h \in \hat{V}_h^k, \tag{3.25}$$

$$\hat{a}_h(\hat{v}_h, \hat{w}_h) \le \beta^{-1}\|\hat{v}_h\|_{\hat{a}_h}\|\hat{w}_h\|_{\hat{a}_h}, \qquad \forall (\hat{v}_h, \hat{w}_h) \in \hat{V}_h^k \times \hat{V}_h^k. \tag{3.26}$$

Owing to the Lax–Milgram Lemma, we infer that the cell-face HHO solution operator $\hat{T}_h : L^2(\Omega) \to \hat{V}_{h,0}^k$ introduced in (3.15) is indeed well-defined. For later use in the analysis of the eigenvalue problem, we now establish a stability property for $\hat{T}_h$.

Lemma 3.2 (Stability of $\hat{T}_h$)**.** *There is C so that*

$$\|\hat{T}_h(\phi)\|_{\hat{a}_h} \le C\|\phi\|_{L^2(\Omega)}, \qquad \forall \phi \in L^2(\Omega). \tag{3.27}$$

Proof. Let $\phi \in L^2(\Omega)$ and let us write $\hat{T}_h(\phi) = (u_\mathcal{K}, u_\mathcal{F})$ with $u_\mathcal{K} \in V_\mathcal{K}^k$ and $u_\mathcal{F} \in V_{\mathcal{F},0}^k$. Using the coercivity property (3.25), the definition (3.15) of the solution operator $\hat{T}_h$, that of the bilinear form b, and the Cauchy–Schwarz inequality leads to

$$\beta\|\hat{T}_h(\phi)\|_{\hat{a}_h}^2 \le \hat{a}_h(\hat{T}_h(\phi), \hat{T}_h(\phi)) = b(\phi, u_\mathcal{K}) \le \|\phi\|_{L^2(\Omega)}\|u_\mathcal{K}\|_{L^2(\Omega)}. \tag{3.28}$$

On the broken polynomial space $V_\mathcal{K}^k$, we can apply the following discrete Poincaré inequality which has been derived in the discontinuous Galerkin context in [4, 10, 24]:

$$C_{\mathrm{P,dG}}\|u_\mathcal{K}\|_{L^2(\Omega)} \le \left(\sum_{K\in\mathcal{K}} \|\nabla u_K\|_{L^2(K)}^2 + \sum_{F\in\mathcal{F}} h_F^{-1}\|[\![u_\mathcal{K}]\!]_F\|_{L^2(F)}^2\right)^{\frac{1}{2}},$$

with $C_{\mathrm{P,dG}} > 0$ uniform with respect to the mesh-size h, and where $[\![u_\mathcal{K}]\!]_F$ denotes the jump of $u_\mathcal{K}$ across F if F is an interface ($F \in \mathcal{F}^{\mathrm{i}}$) or the value of $u_\mathcal{K}$ on F if F is a boundary face ($F \in \mathcal{F}^{\mathrm{b}}$). If $F \in \mathcal{F}^{\mathrm{i}}$, we have $[\![u_\mathcal{K}]\!]_F = u_{K_1}|_F - u_{K_2}|_F$ where K_1, K_2 are the two mesh cells sharing F (the sign of the jump is irrelevant in what follows), and we can therefore write $[\![u_\mathcal{K}]\!]_F = (u_{K_1} - u_F)|_F - (u_{K_2} - u_F)|_F$ where u_F is the component of $u_\mathcal{F}$ attached to F. If $F \in \mathcal{F}^{\mathrm{b}}$, we have $[\![u_\mathcal{K}]\!]_F = u_{K_1}|_F$ where K_1 is the unique mesh

cell sharing F with $\partial\Omega$, and we can therefore write $[\![u_{\mathcal{K}}]\!]_F = (u_{K_1} - u_F)|_F$ since $u_F \equiv 0$ (recall that $u_{\mathcal{F}} \in V^k_{\mathcal{F},0}$). Recalling the definition (3.23) of the $\|\cdot\|_{\hat{a}_h}$-norm, that of $\tau_{\partial K}$ given just below (3.5), and using the triangle inequality, we infer that

$$\|u_{\mathcal{K}}\|_{L^2(\Omega)} \le C\|(u_{\mathcal{K}}, u_{\mathcal{F}})\|_{\hat{a}_h} = C\|\hat{T}_h(\phi)\|_{\hat{a}_h}.$$

Combining this bound with (3.28), we obtain the assertion. □

An important tool in the analysis of HHO methods is the global reduction operator $\hat{I}^k_h : H^1_0(\Omega) \to \hat{V}^k_{h,0}$ defined such that, for all $v \in H^1_0(\Omega)$,

$$\hat{I}^k_h(v) = (\Pi^k_{\mathcal{K}}(v), \Pi^k_{\mathcal{F}}(v)) := ((\Pi^k_K(v))_{K\in\mathcal{K}}, (\Pi^k_F(v))_{F\in\mathcal{F}}) \in \hat{V}^k_{h,0}, \tag{3.29}$$

where Π^k_K and Π^k_F denote the L^2-orthogonal projectors onto $\mathbb{P}^k_d(K)$ and $\mathbb{P}^k_{d-1}(F)$, respectively (for simplicity, the trace operator is omitted for $\Pi^k_{\mathcal{F}}$). We also define the local reduction operator $\hat{I}_K : H^1(K) \to \hat{V}^k_K$ such that, for all $v \in H^1(K)$,

$$\hat{I}_K(v) = (\Pi^k_K(v), \Pi^k_{\partial K}(v)) = (\Pi^k_K(v), (\Pi^k_F(v))_{F\in\mathcal{F}_{\partial K}}) \in \hat{V}^k_K. \tag{3.30}$$

Recalling the local reconstruction operator $p^{k+1}_K : \hat{V}^k_K \to \mathbb{P}^{k+1}_d(K)$ defined in (3.3), [26, Lemma 3] shows that

$$e^{k+1}_K := p^{k+1}_K \circ \hat{I}^k_K : H^1(K) \to \mathbb{P}^{k+1}_d(K), \tag{3.31}$$

is the elliptic projector, i.e., for all $v \in H^1(K)$, $e^{k+1}_K(v)$ is the unique polynomial in $\mathbb{P}^{k+1}_d(K)$ such that $(\nabla(e^{k+1}_K(v) - v), \nabla w)_{L^2(K)} = 0$ for all $w \in \mathbb{P}^{k+1}_d(K)$ and $(e^{k+1}_K(v) - v, 1)_{L^2(K)} = 0$. For two functions $v, w \in H^1(K)$, the above orthogonality condition on the gradient implies that

$$(\nabla(e^{k+1}_K(v) - v), \nabla(e^{k+1}_K(w) - w))_{L^2(K)} = (\nabla v, \nabla w)_{L^2(K)} - (\nabla e^{k+1}_K(v), \nabla e^{k+1}_K(w))_{L^2(K)}. \tag{3.32}$$

Lemma 3.3 (Discrete error estimate)**.** *There is C such that*

$$\|\hat{T}_h(\phi) - \hat{I}_h(T(\phi))\|_{\hat{a}_h} \le Ch^t\|T(\phi)\|_{H^{1+t}(\Omega)}, \tag{3.33}$$

for all $t \in [s, k+1]$, and all $\phi \in L^2(\Omega)$ such that $T(\phi) \in H^{1+t}(\Omega)$; here, $s > \frac{1}{2}$ is the smoothness index resulting from the elliptic regularity theory.

Proof. Let $t \in [s, k+1]$, and let $\phi \in L^2(\Omega)$ be such that $T(\phi) \in H^{1+t}(\Omega)$. Proceeding as in the proof of [26, Theorem 8], we infer that

$$\|\hat{T}_h(\phi) - \hat{I}_h(T(\phi))\|_{\hat{a}_h} \le C \sup_{\substack{\hat{w}_h\in\hat{V}^k_{h,0}\\ \|\hat{w}_h\|_{\hat{a}_h}=1}} |\delta_h(\hat{w}_h)| =: C\,\|\delta_h\|_{(\hat{V}^k_{h,0})'},$$

with the consistency error $\delta_h(\hat{w}_h)$ such that

$$\begin{aligned}\delta_h(\hat{w}_h) = &\sum_{K\in\mathcal{K}} (\nabla\xi_K, \nabla w_K)_{L^2(K)} + (\nabla\xi_K\cdot\boldsymbol{n}_K, w_{\partial K} - w_K)_{L^2(\partial K)}\\ &+ (\tau_{\partial K} S^k_{\partial K}(\hat{I}_K(u)), S^k_{\partial K}(\hat{w}_K))_{L^2(\partial K)},\end{aligned}$$

and the shorthand notation $\xi_K \coloneqq e^{k+1}_K(u) - u$ and $u = T(\phi)$ (we have used $s > \frac{1}{2}$ in writing the second summand in the above right-hand side). Using the Cauchy–Schwarz inequality and recalling the definition of the norm $\|\hat{w}_h\|_{\hat{a}_h}$, we obtain

$$\|\delta_h\|_{(\hat{V}^k_{h,0})'} \le C\left(\sum_{K\in\mathcal{K}} \|\nabla\xi_K\|^2_{L^2(K)} + h_K\|\nabla\xi_K\|^2_{L^2(\partial K)} + h_K^{-1}\|S^k_{\partial K}(\hat{I}_K(u))\|^2_{L^2(\partial K)}\right)^{\frac{1}{2}}.$$

Recalling the definition (3.4) of the stabilization operator $S^k_{\partial K}$ and the property (3.31), we obtain that

$$\begin{aligned}S^k_{\partial K}(\hat{I}_K(u)) &= \Pi^k_{\partial K}(\Pi^k_{\partial K}(u) - \gamma_{\partial K}(e^{k+1}_K(u))) - \gamma_{\partial K}(\Pi^k_K(\Pi^k_{\partial K}(u) - e^{k+1}_K(u)))\\ &= \Pi^k_{\partial K}(\gamma_{\partial K}(u - e^{k+1}_K(u))) - \gamma_{\partial K}(\Pi^k_K(u - e^{k+1}_K(u)))\\ &= -\Pi^k_{\partial K}(\gamma_{\partial K}(\xi_K)) + \gamma_{\partial K}(\Pi^k_K(\xi_K)).\end{aligned}$$

We then have

$$\begin{aligned}\|S^k_{\partial K}(\hat{I}_K(u))\|_{L^2(\partial K)} &\le \|\xi_K\|_{L^2(\partial K)} + \|\Pi^k_K(\xi_K)\|_{L^2(\partial K)}\\ &\le \|\xi_K\|_{L^2(\partial K)} + Ch_K^{-\frac{1}{2}}\|\xi_K\|_{L^2(K)}\\ &\le C'(h_K^{-\frac{1}{2}}\|\xi_K\|_{L^2(K)} + h_K^{\frac{1}{2}}\|\nabla\xi_K\|_{L^2(K)})\\ &\le C'' h_K^{\frac{1}{2}}\|\nabla\xi_K\|_{L^2(K)},\end{aligned}$$

where we used a triangle inequality and the L^2-stability of $\Pi^k_{\partial K}$ in the first line, a discrete trace inequality and the L^2-stability of Π^k_K in the second line, a multiplicative trace inequality in the third line, and the the Poincaré–Steklov inequality on K in the fourth line (that is, $\|\xi_K\|_{L^2(K)} \le C''' h_K\|\nabla\xi_K\|_{L^2(K)}$ since ξ_K has zero mean-value in K by construction). We conclude that $h_K^{-\frac{1}{2}}\|S^k_{\partial K}(\hat{I}_K(u))\|_{L^2(\partial K)} \le C\|\nabla\xi_K\|_{L^2(K)}$ for some generic constant C, and therefore, we have

$$\|\delta_h\|_{(\hat{V}^k_{h,0})'} \le C\left(\sum_{K\in\mathcal{K}} \|\nabla\xi_K\|^2_{L^2(K)} + h_K\|\nabla\xi_K\|^2_{L^2(\partial K)}\right)^{\frac{1}{2}}.$$

Finally, invoking the approximation properties of the elliptic projector on all the mesh cells leads to the assertion. □

4 Error analysis for the eigenvalue problem

The goal of this section is to perform the error analysis of the discrete eigenvalue problem (3.12) by using the abstract theory outlined in Section 2.2 in the Hilbert space $L = L^2(\Omega)$. Let $T, T^* : L^2(\Omega) \to H_0^1(\Omega) \subset L^2(\Omega)$ be the exact solution and adjoint solution operators defined in Section 2.1 ($T = T^*$, i.e., T is selfadjoint, in the present symmetric setting). Let $T_{\mathcal{K}} : L \to V_{\mathcal{K}}^k \subset L$ be the discrete HHO solution operator defined in (3.19). Its adjoint operator $T_{\mathcal{K}}^* : L \to V_{\mathcal{K}} \subset L$ is defined so that, for all $\psi \in L$, $T_{\mathcal{K}}^*(\psi) \in V_{\mathcal{K}}$ is the unique solution of

$$a_{\mathcal{K}}(w_{\mathcal{K}}, T_{\mathcal{K}}^*(\psi)) = b(w_{\mathcal{K}}, \psi), \qquad \forall w_{\mathcal{K}} \in V_{\mathcal{K}}^k. \tag{4.1}$$

Owing to the symmetry of the bilinear forms $a_{\mathcal{K}}$ and b, we have $T_{\mathcal{K}} = T_{\mathcal{K}}^*$ in the present setting, i.e., $T_{\mathcal{K}}$ is selfadjoint. We keep as before a distinct notation to allow for more generality, and we also set $\hat{T}_h^\dagger : L \to \hat{V}_{h,0}^k$ so that $\hat{T}_h^\dagger(\psi) = (T_{\mathcal{K}}^*(\psi), (Z_{\mathcal{F},0}^\dagger \circ T_{\mathcal{K}}^*)(\psi))$ for all $\psi \in L$. Proceeding as in Lemma 3.1, we conclude that

$$\hat{a}_h(\hat{w}_h, \hat{T}_h^\dagger(\psi)) = b(w_{\mathcal{K}}, \psi), \qquad \forall \hat{w}_h = (w_{\mathcal{K}}, w_{\mathcal{F}}) \in \hat{V}_{h,0}^k. \tag{4.2}$$

In the present symmetric setting, we have $\hat{T}_h = \hat{T}_h^\dagger$ with $\hat{T}_h$ defined in (3.15). Finally, the elliptic regularity theory implies that there is a real number $s \in (\frac{1}{2}, 1]$ so that $T, T^* \in \mathcal{L}(L^2(\Omega); H^{1+s}(\Omega))$, with operator norm denoted by C_s.

4.1 Preliminary results

To verify that we can apply the abstract theory from Section 2.2, let us show that $T_{\mathcal{K}}$ converges to T in operator norm as the mesh-size h tends to zero, i.e., that (2.10) holds true.

Lemma 4.1 (Bound on $L \times L$)**.** *The following holds true:*

$$\sup_{(\phi,\psi)\in L\times L} |((T - T_{\mathcal{K}})(\phi), \psi)_L| \le C h^s \|\phi\|_L \|\psi\|_L. \tag{4.3}$$

where $s \in (\frac{1}{2}, 1]$ is the smoothness index associated with the elliptic regularity theory. Consequently, we have $\|T - T_{\mathcal{K}}\|_{\mathcal{L}(L;L)} \to 0$ as $h \to 0$.

Proof. For all $\phi, \psi \in L$, we have

$$\begin{aligned}
&((T - T_{\mathcal{K}})(\phi), \psi)_L \\
&= (T(\phi), \psi)_L - b(T_{\mathcal{K}}(\phi), \psi) \\
&= (T(\phi), \psi)_L - a_{\mathcal{K}}(T_{\mathcal{K}}(\phi), T_{\mathcal{K}}^*(\psi)) \\
&= (T(\phi), \psi)_L - \hat{a}_h(\hat{T}_h(\phi), \hat{T}_h^\dagger(\psi)) \\
&= (T(\phi), \psi)_L - \hat{a}_h(\hat{I}_h^k(T(\phi)), \hat{T}_h^\dagger(\psi)) + \hat{a}_h(\hat{I}_h^k(T(\phi)) - \hat{T}_h(\phi), \hat{T}_h^\dagger(\psi)) \\
&= (T(\phi) - \Pi_{\mathcal{K}}^k(T(\phi)), \psi)_L + \hat{a}_h(\hat{I}_h^k(T(\phi)) - \hat{T}_h(\phi), \hat{T}_h^\dagger(\psi)),
\end{aligned} \tag{4.4}$$

where we have used the definition of the bilinear form b in the first line of the right-hand side, the definition (4.1) of $T^*_{\mathcal{K}}$ in the second line, the definition (3.18) of $a_{\mathcal{K}}$ and Lemma 3.1 in the third line, a simple algebraic manipulation in the fourth line, and the property (4.2) and the definition (3.29) of $\hat{I}^k_h$ in the fifth line. Let us call S_1, S_2 the two summands on the right-hand side of (4.4). Owing to the elliptic regularity theory and the approximation properties of the projector $\Pi^k_{\mathcal{K}}$ (with $k \geq 0$), we obtain that

$$|S_1| \leq Ch|T(\phi)|_{H^1(\Omega)}\|\psi\|_L.$$

Since $|T(\phi)|_{H^1(\Omega)} \leq \|T(\phi)\|_{H^{1+s}(\Omega)} \leq C_s\|\phi\|_L$, we infer that

$$|S_1| \leq Ch\|\phi\|_L\|\psi\|_L.$$

To bound S_2, we use the boundedness property (3.26) of $\hat{a}_h$ followed by the error estimate from Lemma 3.3 (with $t = s$) and the stability property of $\hat{T}^\dagger_h = \hat{T}_h$ from Lemma 3.2 to infer that

$$|S_2| \leq Ch^s\|T(\phi)\|_{H^{1+s}(\Omega)}\|\psi\|_L \leq CC_sh^s\|\phi\|_L\|\psi\|_L.$$

Combining the bounds on S_1 and S_2 and observing that $s \leq 1$ concludes the proof. □

Let $\mu \in \sigma(T) \setminus \{0\}$ with ascent α and algebraic multiplicity m. To quantify the smoothness of the functions in the subspaces G_μ and G^*_μ defined in (2.11), we assume that there is a real number $t \in [s, k+1]$ and a constant C_t so that

$$\begin{aligned} \|\phi\|_{H^{1+t}(\Omega)} + \|T(\phi)\|_{H^{1+t}(\Omega)} &\leq C_t\|\phi\|_L, \qquad \forall \phi \in G_\mu, \\ \|\psi\|_{H^{1+t}(\Omega)} + \|T^*(\psi)\|_{H^{1+t}(\Omega)} &\leq C_t\|\psi\|_L, \qquad \forall \psi \in G^*_\mu. \end{aligned} \tag{4.5}$$

Note that t depends on μ, but we just write t instead of t_μ to alleviate the notation. If $t = s$, functions in G_μ and G^*_μ do not provide additional smoothness with respect to that resulting from the elliptic regularity theory. In general, functions in G_μ and G^*_μ are smoother, and one has $t > s$. The case $t = k+1$ leads to optimal error estimates, see Remark 4.7 below.

Lemma 4.2 (Bound on $G_\mu \times L$ and $L \times G^*_\mu$)**.** *The following holds true:*

$$\sup_{(\phi,\psi)\in G_\mu\times L} |((T - T_{\mathcal{K}})(\phi), \psi)_L| \leq Ch^t\|\phi\|_L\|\psi\|_L, \tag{4.6}$$

where $t \in [s, k+1]$ is the smoothness index associated with μ. Consequently, we have

$$\|(T - T_{\mathcal{K}})|_{G_\mu}\|_{\mathcal{L}(G_\mu;L)} \leq Ch^t. \tag{4.7}$$

Similar bounds hold for $T^*_{\mathcal{K}}$, and in particular, we have $\|(T - T_{\mathcal{K}})^*|_{G^*_\mu}\|_{\mathcal{L}(G^*_\mu;L)} \leq Ch^t$.

Proof. Owing to symmetry, we only need to prove the statement for $T_{\mathcal{K}}$. Our starting point is (4.4). Owing to the smoothness of the function $T(\phi)$ resulting from (4.5), we infer that

$$|S_1| \leq Ch^{\min(k+1,t+1)}\|T(\phi)\|_{H^{1+t}(\Omega)}\|\psi\|_L \leq CC_th^{\min(k+1,t+1)}\|\phi\|_L\|\psi\|_L.$$

Using similar arguments leads to $|S_2| \leq Ch^t\|\phi\|_L\|\psi\|_L$ and since $t \leq \min(k+1, t+1)$, the assertion follows. □

Lemma 4.3 (Bound on $G_\mu \times G_\mu^*$)**.** *The following holds true:*

$$\sup_{(\phi,\psi)\in G_\mu\times G_\mu^*} |((T-T_{\mathcal{K}})(\phi),\psi)_L| \le Ch^{2t}\|\phi\|_L\|\psi\|_L, \tag{4.8}$$

where $t \in [s, k+1]$ is the smoothness index associated with μ.

Proof. Our starting point is again (4.4), but we can now derive sharper bounds on the two summands S_1 and S_2 by exploiting the smoothness of both ϕ and ψ. On the one hand, we have

$$S_1 = (T(\phi) - \Pi_{\mathcal{K}}^k(T(\phi)),\psi)_L = (T(\phi) - \Pi_{\mathcal{K}}^k(T(\phi)),\psi - \Pi_{\mathcal{K}}^k(\psi))_L,$$

so that

$$|S_1| \le Ch^{2\min(k+1,t+1)}\|T(\phi)\|_{H^{1+t}(\Omega)}\|\psi\|_{H^{1+t}(\Omega)} \le CC_t^2h^{2\min(k+1,t+1)}\|\phi\|_L\|\psi\|_L,$$

where we used the smoothness of the functions $T(\phi)$ and ψ resulting from (4.5). On the other hand, we have

$$\begin{aligned}
S_2 &= \hat{a}_h(\hat{I}_h^k(T(\phi)) - \hat{T}_h(\phi), \hat{T}_h^\dagger(\psi))\\
&= \hat{a}_h(\hat{I}_h^k(T(\phi)) - \hat{T}_h(\phi), \hat{I}_h^k(T^*(\psi))) + \hat{a}_h(\hat{I}_h^k(T(\phi)) - \hat{T}_h(\phi), \hat{T}_h^\dagger(\psi) - \hat{I}_h^k(T^*(\psi)))\\
&= a(T(\phi),T^*(\psi)) - \hat{a}_h(\hat{T}_h(\phi), \hat{I}_h^k(T^*(\psi)))\\
&\quad + \hat{a}_h(\hat{I}_h^k(T(\phi)), \hat{I}_h^k(T^*(\psi))) - a(T(\phi),T^*(\psi))\\
&\quad + \hat{a}_h(\hat{I}_h^k(T(\phi)) - \hat{T}_h(\phi), \hat{T}_h^\dagger(\psi) - \hat{I}_h^k(T^*(\psi)))\\
&= (\phi - \Pi_{\mathcal{K}}^k(\phi), T^*(\psi) - \Pi_{\mathcal{K}}^k(T^*(\psi)))_L\\
&\quad + \hat{a}_h(\hat{I}_h^k(T(\phi)), \hat{I}_h^k(T^*(\psi))) - a(T(\phi),T^*(\psi))\\
&\quad + \hat{a}_h(\hat{I}_h^k(T(\phi)) - \hat{T}_h(\phi), \hat{T}_h^\dagger(\psi) - \hat{I}_h^k(T^*(\psi)))
\end{aligned}$$

where we have used simple algebraic manipulations to derive the second and third identities, and the definition of T together with that of $\hat{T}_h$ and of $\hat{I}_h^k$ to derive the last identity. Let us call $S_{2,1}$, $S_{2,2}$, $S_{2,3}$ the three summands on the right-hand side of the above equation. Reasoning as above while invoking the smoothness of the functions ϕ and $T^*(\psi)$ resulting from (4.5), we infer that

$$|S_{2,1}| \le CC_t^2h^{2\min(k+1,t+1)}\|\phi\|_L\|\psi\|_L.$$

To bound $S_{2,2}$, we observe that

$$\begin{aligned}
S_{2,2} &= \sum_{K\in\mathcal{K}} (\nabla e_K^{k+1}(T(\phi)), \nabla e_K^{k+1}(T^*(\psi)))_{L^2(K)} - (\nabla T(\phi), \nabla T^*(\psi))_{L^2(K)}\\
&\quad + \sum_{K\in\mathcal{K}} (\tau_{\partial K} S_{\partial K}^k(\hat{I}_h^k(T(\phi))), S_{\partial K}^k(\hat{I}_h^k(T^*(\phi))))_{L^2(\partial K)} =: S_{2,2,1} + S_{2,2,2}.
\end{aligned}$$

Since e_K^{k+1} is the elliptic projector, the identity (3.32) implies that

$$S_{2,2,1} = \sum_{K\in\mathcal{K}} -(\nabla(T(\phi) - e_K^{k+1}(T(\phi))), \nabla(T^*(\psi) - e_K^{k+1}(T^*(\psi))))_{L^2(K)},$$

Using Lemma 3.3 and the definition of the $\|\cdot\|_{\hat{a}_h}$-norm, we infer that

$$|S_{2,2,1}| \le Ch^{2t}\|T(\phi)\|_{H^{1+t}(\Omega)}\|T^*(\psi)\|_{H^{1+t}(\Omega)} \le CC_t^2h^{2t}\|\phi\|_L\|\psi\|_L.$$

Moreover, reasoning as in the end of the proof of Lemma 3.3, we obtain that

$$|S_{2,2,2}| \le Ch^{2t}\|T(\phi)\|_{H^{1+t}(\Omega)}\|T^*(\psi)\|_{H^{1+t}(\Omega)} \le CC_t^2h^{2t}\|\phi\|_L\|\psi\|_L.$$

Hence, we have

$$|S_{2,2}| \le CC_t^2h^{2t}\|\phi\|_L\|\psi\|_L.$$

Finally, the bound on $S_{2,3}$ results from the boundedness property (3.26) of $\hat{a}_h$ and the error estimate from Lemma 3.3 which lead to

$$|S_{2,3}| \le Ch^{2t}\|T(\phi)\|_{H^{1+t}(\Omega)}\|T^*(\psi)\|_{H^{1+t}(\Omega)} \le CC_t^2h^{2t}\|\phi\|_L\|\psi\|_L.$$

Collecting the above estimates concludes the proof. □

4.2 Main results

We can now present our main results. Let $\mu \in \sigma(T) \setminus \{0\}$ with ascent α and algebraic multiplicity m. Owing to the convergence result from Lemma 4.1, there are m eigenvalues of $T_\mathcal{K}$, denoted $\mu_{h,1}, \dots, \mu_{h,m}$, that converge to μ as $h \to 0$. Let $\langle\mu_h\rangle = \sum_{j=1}^m \mu_{h,j}$ denote the arithmetic mean of these eigenvalues.

Theorem 4.4 (Error estimate on eigenvalues and eigenfunctions in L)**.** *Assume that there is $t \in [s, k+1]$ so that the smoothness property (4.5) holds true, where $s > \frac{1}{2}$ is the smoothness index resulting from the elliptic regularity theory. Then there is C, depending on μ (and on the mesh regularity, the polynomial degree k and the domain Ω) but independent of the mesh-size h, such that*

$$\max_{1\le j\le m} |\mu - \mu_{h,j}|^\alpha + |\mu - \langle\mu_h\rangle| \le Ch^{2t}. \tag{4.9}$$

Furthermore, let $u_{\mathcal{K},j} \in V_\mathcal{K}^k$ be a unit vector in $\ker(\mu_{h,j}I - T_\mathcal{K})^\ell$ for some positive integer $\ell \le \alpha$. Then, for any integer m with $\ell \le m \le \alpha$, there is a unit vector $u_m \in \ker(\mu I - T)^m \subset G_\mu$ such that

$$\|u_m - u_{\mathcal{K},j}\|_L \le Ch^{t\frac{m-\ell+1}{\alpha}}. \tag{4.10}$$

Proof. Combining the results from Lemma 4.2, and Lemma 4.3 with Theorem 2.1 and Theorem 2.3 completes the proof. □

Remark 4.5 (Error estimate on eigenvalues)**.** Since the eigenvalues λ and λ_h associated with (2.2) and (3.12), respectively, are such that $\lambda = \mu^{-1}$ and $\lambda_h = \mu_h^{-1}$, we infer that the same estimate as (4.9) holds true for the error between λ and λ_h.

Corollary 4.6 (Eigenfunction error estimate in H^1)**.** *Assume that $\alpha = m = 1$ for the exact eigenvalue μ. Since μ_h is simple, we drop the index j for the approximate eigenfunction $u_{\mathcal{K}}$ and we set $\hat{u}_h = (u_{\mathcal{K}}, Z_{\mathcal{F},0}(u_{\mathcal{K}}))$. Then the following holds true:*

$$\hat{a}_h(\hat{u}_h - \hat{I}_h(u), \hat{u}_h - \hat{I}_h(u))^{\frac{1}{2}} \le Ch^t. \tag{4.11}$$

Consequently, we have

$$\left(\sum_{K\in\mathcal{K}} \|\nabla(u - p_K^{k+1}(\hat{u}_K))\|_{L^2(K)}^2 \right)^{\frac{1}{2}} \le Ch^t. \tag{4.12}$$

Proof. Since $\alpha = m = 1$, we have $\ell = 1$ in (4.10); moreover, $\mu_h = \lambda_h^{-1}$ is also simple and we drop the index j. The bound (4.10) becomes $\|u - u_{\mathcal{K}}\|_L \le Ch^t$. We observe that

$$\begin{aligned}
\lambda_h(u_{\mathcal{K}}, u)_L &= \lambda_h(u_{\mathcal{K}}, \Pi_{\mathcal{K}}^k(u))_L = \lambda_h b(u_{\mathcal{K}}, \Pi_{\mathcal{K}}^k(u)) = a_{\mathcal{K}}(u_{\mathcal{K}}, \Pi_{\mathcal{K}}^k(u)) \\
&= \hat{a}_h((u_{\mathcal{K}}, Z_{\mathcal{F},0}(u_{\mathcal{K}})), (\Pi_{\mathcal{K}}^k(u), Z_{\mathcal{F},0}^\dagger(\Pi_{\mathcal{K}}^k(u))) \\
&= \hat{a}_h((u_{\mathcal{K}}, Z_{\mathcal{F},0}(u_{\mathcal{K}})), (\Pi_{\mathcal{K}}^k(u), Z_{\mathcal{F},0}^\dagger(\Pi_{\mathcal{K}}^k(u))) \\
&\quad + \hat{a}_h((u_{\mathcal{K}}, Z_{\mathcal{F},0}(u_{\mathcal{K}})), (0, \Pi_{\mathcal{F}}^k(u) - Z_{\mathcal{F},0}^\dagger(\Pi_{\mathcal{K}}^k(u))) \\
&= \hat{a}_h(\hat{u}_h, \hat{I}_h(u)),
\end{aligned}$$

where we have used the definition of $\Pi_{\mathcal{K}}$ and (3.21) in the first line, the definition (3.18) of $\hat{a}_h$ in the second line, the property (3.16) of $Z_{\mathcal{F},0}$ in the third line, and the definition of $\hat{I}_h$ in the last line. Setting $\delta_u := \hat{a}_h(\hat{I}_h(u), \hat{I}_h(u)) - a(u,u)$ and recalling the normalization $\|u\|_L = \|u_{\mathcal{K}}\|_L = 1$, we infer that

$$\begin{aligned}
\hat{a}_h(\hat{u}_h - \hat{I}_h(u), \hat{u}_h - \hat{I}_h(u)) &= \hat{a}_h(\hat{u}_h, \hat{u}_h) - 2\hat{a}_h(\hat{u}_h, \hat{I}_h(u)) + \hat{a}_h(\hat{I}_h(u), \hat{I}_h(u)) \\
&= \lambda_h \|u_{\mathcal{K}}\|_L^2 - 2\lambda_h(u_{\mathcal{K}}, u)_L + \lambda_h \|u\|_L^2 - (\lambda_h - \lambda)\|u\|_L^2 + \delta_u \\
&= \lambda_h \|u_{\mathcal{K}} - u\|_L^2 + \lambda_h - \lambda + \delta_u,
\end{aligned}$$

which is a generalization of the Pythagorean eigenvalue error identity (see [41]) in the HHO context. The bound (4.11) then follows from the bounds derived in Theorem 4.4. Finally, the bound (4.12) follows from the definition of the bilinear form $\hat{a}_h$, the identity (3.31), the triangle inequality, and the approximation properties of the elliptic projector. □

Remark 4.7 (Optimal convergence)**.** If $t = k + 1$, we recover a convergence of order h^{2k+2} for the eigenvalues and of order k^{k+1} for the eigenfunctions in the H^1-seminorm.

5 Numerical experiments

In this section, we first verify the error estimates from Section 4 for eigenvalues and smooth eigenfunctions approximated by the HHO method in 1D (unit interval) and in

2D (unit square). We then report extra-superconvergence results for 1D uniform meshes for a particular choice of the stabilization parameter. Finally, we present convergence results on an L-shaped domain (which includes the case of a non-smooth eigenfunction) as well as on the unit disk. We consider the eigenvalues λ and λ_h associated with (2.2) and (3.12), respectively; both eigenvalues are sorted in increasing order as $\lambda_1 < \lambda_2 \ldots$ and $\lambda_{1,h} < \lambda_{2,h} \ldots$, and we report the normalized eigenvalue errors $\frac{|\lambda_j - \lambda_{h,j}|}{\lambda_j}$.

k	N	first mode		second mode		fourth mode		eighth mode	
		error	order	error	order	error	order	error	order
0	10	3.19e-2	—	1.17e-1	—	3.50e-1	—	6.99e-1	—
	20	8.16e-3	1.97	3.19e-2	1.87	1.17e-1	1.58	3.50e-1	1.00
	40	2.05e-3	1.99	8.16e-3	1.97	3.19e-2	1.87	1.17e-1	1.58
	80	5.14e-4	2.00	2.05e-3	1.99	8.16e-3	1.97	3.19e-2	1.87
	160	1.28e-4	2.00	5.14e-4	2.00	2.05e-3	1.99	8.16e-3	1.97
	320	3.21e-5	2.00	1.28e-4	2.00	5.14e-4	2.00	2.05e-3	1.99
1	10	1.10e-4	—	1.81e-3	—	3.25e-2	—	4.01e-1	—
	20	6.78e-6	4.01	1.10e-4	4.05	1.81e-3	4.16	3.25e-2	3.63
	40	4.23e-7	4.00	6.78e-6	4.01	1.10e-4	4.05	1.81e-3	4.16
	80	2.64e-8	4.00	4.23e-7	4.00	6.78e-6	4.01	1.10e-4	4.05
	160	1.65e-9	4.00	2.64e-8	4.00	4.23e-7	4.00	6.78e-6	4.01
	320	1.01e-10	4.03	1.65e-9	4.00	2.64e-8	4.00	4.23e-7	4.00
2	10	1.15e-7	—	7.52e-6	—	5.28e-4	—	6.08e-2	—
	20	1.79e-9	6.01	1.15e-7	6.03	7.52e-6	6.13	5.28e-4	6.85
	40	2.78e-11	6.01	1.79e-9	6.01	1.15e-7	6.03	7.52e-6	6.13
	80	9.88e-14	8.14	2.78e-11	6.01	1.79e-9	6.01	1.15e-7	6.03
3	5	1.56e-8	—	4.23e-6	—	1.59e-3	—	5.09e-1	—
	10	6.01e-11	8.02	1.56e-8	8.09	4.23e-6	8.55	1.59e-3	8.32
	20	1.06e-13	9.14	6.00e-11	8.02	1.56e-8	8.09	4.23e-6	8.55

Table 1: Unit interval, relative eigenvalue errors, $\eta = 1$.

5.1 Smooth eigenfunctions in 1D and 2D unit domains

Let $\Omega = (0,1)$ or $\Omega = (0,1) \times (0,1)$ be the unit interval in 1D or the unit square in 2D, respectively. The 1D problem (2.1) has exact eigenvalues $\lambda_j = j^2\pi^2$ and corresponding eigenfunctions $u_j(x) = \sin(j\pi x)$ with $j = 1, 2, \cdots$, whereas the 2D problem (2.1) has exact eigenvalues $\lambda_{jk} = \pi^2(j^2 + k^2)$ and eigenfunctions $u_{jk}(x, y) = \sin(j\pi x)\sin(k\pi y)$ with $j, k = 1, 2, \cdots$. We discretize the unit interval uniformly with $N = 10, 20, 40, 80, 160, 320$

elements and the unit square uniformly with $N \times N$ squares with $N = 4, 8, 16, 32, 64, 128$. The default stabilization parameter of the HHO method is $\eta = 1$. The relative eigenvalue errors are reported in Table 1 in 1D and in Table 2 in 2D for the first, second, fourth, and eighth eigenvalues and for the polynomial degrees $k = 0, 1, 2, 3$. These tables show good agreement with the convergence order predicted by Theorem 4.4, i.e., the convergence order for the eigenvalues is indeed h^{2k+2}. The H^1-seminorm errors on the first, second, fourth, and eighth eigenfunctions in 1D are reported in Table 3. We observe a good agreement with the convergence order predicted by Corollary 4.6, that is, the convergence order for the eigenfunctions in the H^1-seminorm is indeed h^{k+1}.

k	N	first mode		second mode		fourth mode		eighth mode	
		error	order	error	order	error	order	error	order
0	4	2.51e-1	—	5.11e-1	—	6.36e-1	—	7.39e-1	—
	8	7.70e-2	1.70	2.16e-1	1.24	2.51e-1	1.34	4.08e-1	0.86
	16	2.04e-2	1.92	6.57e-2	1.72	7.70e-2	1.70	1.33e-1	1.61
	32	5.18e-3	1.98	1.74e-2	1.92	2.04e-2	1.92	3.73e-2	1.84
	64	1.30e-3	1.99	4.41e-3	1.98	5.18e-3	1.98	9.62e-3	1.96
	128	3.25e-4	2.00	1.11e-3	1.99	1.30e-3	1.99	2.42e-3	1.99
1	4	2.27e-2	—	1.62e-1	—	3.32e-1	—	5.10e-1	—
	8	1.45e-3	3.97	9.75e-3	4.06	2.27e-2	3.87	6.35e-2	3.01
	16	9.15e-5	3.98	5.96e-4	4.03	1.45e-3	3.97	3.90e-3	4.02
	32	5.74e-6	3.99	3.71e-5	4.00	9.15e-5	3.98	2.45e-4	3.99
	64	3.59e-7	4.00	2.32e-6	4.00	5.74e-6	3.99	1.54e-5	4.00
	128	2.25e-8	4.00	1.45e-7	4.00	3.59e-7	4.00	9.61e-7	4.00
2	4	5.71e-4	—	8.46e-3	—	4.91e-2	—	2.31e-1	—
	8	8.63e-6	6.05	1.07e-4	6.30	5.71e-4	6.43	2.33e-3	6.64
	16	1.34e-7	6.01	1.62e-6	6.05	8.63e-6	6.05	3.34e-5	6.12
	32	2.09e-9	6.00	2.51e-8	6.01	1.34e-7	6.01	5.14e-7	6.02
	64	3.26e-11	6.00	3.92e-10	6.00	2.09e-9	6.00	8.01e-9	6.00
3	4	6.48e-6	—	2.18e-4	—	2.20e-3	—	2.42e-2	—
	8	2.43e-8	8.06	7.13e-7	8.25	6.48e-6	8.41	4.24e-5	9.15
	16	9.46e-11	8.01	2.69e-9	8.05	2.43e-8	8.06	1.52e-7	8.13

Table 2: Unit square, relative eigenvalue errors, $\eta = 1$.

5.2 Superconvergence with rate $(2k + 4)$ in 1D

We now report some striking numerical results for the HHO method with the stabilization parameter $\eta = 2k + 3$ on 1D uniform meshes. In this case, we observe numerically two

k	N	first mode		second mode		fourth mode		eighth mode	
		error	order	error	order	error	order	error	order
	10	2.08e-1	—	9.87e-1	—	4.39e0	—	1.61e+1	—
	20	1.02e-1	1.03	4.16e-1	1.25	1.97e0	1.15	8.78e0	0.88
0	40	5.05e-2	1.01	2.03e-1	1.03	8.32e-1	1.25	3.95e0	1.15
	80	2.52e-2	1.00	1.01e-1	1.01	4.06e-1	1.03	1.66e0	1.25
	160	1.26e-2	1.00	5.04e-2	1.00	2.02e-1	1.01	8.13e-1	1.03
	10	8.17e-3	—	9.87e-2	—	3.33e0	—	1.54e+1	—
	20	2.04e-3	2.00	1.63e-2	2.60	1.97e-1	4.08	6.67e0	1.21
1	40	5.11e-4	2.00	4.09e-3	2.00	3.27e-2	2.60	3.95e-1	4.08
	80	1.28e-4	2.00	1.02e-3	2.00	8.17e-3	2.00	6.53e-2	2.60
	160	3.19e-5	2.00	2.55e-4	2.00	2.04e-3	2.00	1.63e-2	2.00
	10	2.17e-4	—	4.36e-3	—	1.52e0	—	1.54e+1	—
	20	2.71e-5	3.00	4.34e-4	3.33	8.71e-3	7.45	3.05e0	2.33
2	40	3.39e-6	3.00	5.42e-5	3.00	8.67e-4	3.33	1.74e-2	7.45
	80	4.24e-7	3.00	6.78e-6	3.00	1.08e-4	3.00	1.73e-3	3.33
	160	5.30e-8	3.00	8.47e-7	3.00	1.36e-5	3.00	2.17e-4	3.00
	10	4.29e-6	—	2.06e-4	—	1.85e0	—	1.38e+1	—
	20	2.68e-7	4.00	8.58e-6	4.59	4.13e-4	12.13	3.69e0	1.90
3	40	1.68e-8	4.00	5.37e-7	4.00	1.72e-5	4.59	8.26e-4	12.13
	80	1.05e-9	4.00	3.35e-8	4.00	1.07e-6	4.00	3.43e-5	4.59
	160	7.50e-11	3.81	2.10e-9	4.00	6.71e-8	4.00	2.15e-6	4.00

Table 3: Unit interval, H^1-seminorm errors on eigenfunctions, $\eta = 1$.

extra orders in the convergence of the relative eigenvalue errors, i.e., these errors now converge with order h^{2k+4}, as reported in Table 4. We thus obtain relative eigenvalue errors close to machine precision already on relatively coarse meshes. Moreover, we observe numerically (results are not reported for brevity) that taking values different from $2k + 3$ for the stabilization parameter does not improve the relative eigenvalue errors. We also point out that the choice $\eta = 2k + 3$ does not increase the convergence order of the eigenfunctions. In 2D, we observe that the choice $\eta = 2k + 3$ improves the approximation significantly in the sense of a much smaller constant C in (4.9) but with order h^{2k+2}. The results are reported in Table 5 (compare with Table 2). The theoretical analysis of the above observations will be the subject of future work.

k	N	first mode		second mode		fourth mode		eighth mode	
		error	order	error	order	error	order	error	order
	10	4.07e-5	—	6.59e-4	—	1.10e-2	—	1.80e-1	—
	20	2.54e-6	4.00	4.07e-5	4.02	6.59e-4	4.05	1.10e-2	4.04
	40	1.59e-7	4.00	2.54e-6	4.00	4.07e-5	4.02	6.59e-4	4.05
0	80	9.91e-9	4.00	1.59e-7	4.00	2.54e-6	4.00	4.07e-5	4.02
	160	6.19e-10	4.00	9.91e-9	4.00	1.59e-7	4.00	2.54e-6	4.00
	320	4.18e-11	3.89	6.21e-10	4.00	9.91e-9	4.00	1.59e-7	4.00
	5	1.66e-6	—	1.13e-4	—	1.19e-2	—	1.74e-2	—
	10	2.55e-8	6.02	1.66e-6	6.09	1.13e-4	6.72	1.19e-2	0.54
1	20	3.98e-10	6.00	2.55e-8	6.02	1.66e-6	6.09	1.13e-4	6.72
	40	5.95e-12	6.06	3.98e-10	6.00	2.55e-8	6.02	1.66e-6	6.09
	4	9.18e-9	—	2.42e-6	—	1.34e-2	—	5.20e-1	—
2	8	3.57e-11	8.01	9.18e-9	8.04	2.42e-6	12.43	1.34e-2	5.28
	16	1.04e-13	8.42	3.57e-11	8.01	9.18e-9	8.04	2.42e-6	12.43

Table 4: Unit interval, relative eigenvalue errors, $\eta = 2k + 3$.

5.3 Hexagonal meshes in 2D

To illustrate the fact that the same convergence orders can be obtained if the HHO method is deployed on general meshes, we consider now a quasi-uniform sequence of hexagonal meshes of the unit square; see Figure 1 (also [28]). The coarsest mesh in the sequence ($\ell = 0$) is composed of predominantly hexagonal cells with average diameter 0.065301; the average diameter is halved from one mesh in the sequence to the next mesh. Table 6 shows the relative eigenvalue errors for $k = 0, 1, 2$ with stabilization parameter $\eta = 1$ and $\eta = 2k + 3$ for the first ($j = 1$) and third ($j = 3$) eigenpairs. We observe a convergence of order h^{2k+2}, in agreement with Theorem 4.4. Once again, the choice $\eta = 2k + 3$ for the stabilization parameter does not change the convergence order, but substantially improves the constant C.

5.4 L-shaped domain

We study the Laplacian eigenvalue problem on the L-shaped domain $\Omega = \Omega_0 \backslash \Omega_1$, where $\Omega_0 = (0, 2) \times (0, 2)$ and $\Omega_1 = [1, 2] \times [1, 2]$. The L-shaped domain Ω has a reentrant corner at the point $(1, 1)$, which results in possibly non-smooth eigenfunctions. In fact, the first eigenfunction is in H^{1+t} with $t = \frac{2}{3}$ and the corresponding eigenvalue is $\lambda_1 = 9.6397238440219$ [7]. There are also smooth eigenfunctions. For example, the third eigenfunction is smooth and the corresponding eigenvalue is known exactly to be $\lambda_3 = 2\pi^2$. Figure 2 shows the HHO approximations (with $\eta = 1$) of the first and the third eigenfunctions using quasi-uniform triangulations of Ω.

k	N	first mode		second mode		fourth mode		eighth mode	
		error	order	error	order	error	order	error	order
0	4	4.23e-2	—	1.41e-1	—	1.66e-1	—	3.97e-1	—
	8	1.06e-2	1.99	3.60e-2	1.97	4.23e-2	1.97	7.84e-2	2.34
	16	2.66e-3	2.00	9.04e-3	1.99	1.06e-2	1.99	1.98e-2	1.99
	32	6.65e-4	2.00	2.26e-3	2.00	2.66e-3	2.00	4.96e-3	2.00
	64	1.66e-4	2.00	5.66e-4	2.00	6.65e-4	2.00	1.24e-3	2.00
	128	4.16e-5	2.00	1.41e-4	2.00	1.66e-4	2.00	3.10e-4	2.00
1	4	2.74e-4	—	3.33e-3	—	5.80e-5	—	1.73e-2	—
	8	2.13e-5	3.69	1.69e-4	4.30	2.74e-4	-2.24	1.75e-4	6.63
	16	1.40e-6	3.93	9.93e-6	4.09	2.13e-5	3.69	3.47e-6	5.66
	32	8.82e-8	3.98	6.11e-7	4.02	1.40e-6	3.93	4.41e-7	2.97
	64	5.53e-9	4.00	3.80e-8	4.01	8.82e-8	3.98	3.11e-8	3.83
	128	3.46e-10	4.00	2.37e-9	4.00	5.53e-9	4.00	2.00e-9	3.96
2	4	1.75e-5	—	3.33e-5	—	8.23e-4	—	1.28e-3	—
	8	2.90e-7	5.91	8.50e-7	5.29	1.75e-5	5.56	4.54e-5	4.82
	16	4.60e-9	5.98	1.45e-8	5.87	2.90e-7	5.91	8.01e-7	5.82
	32	7.20e-11	6.00	2.32e-10	5.97	4.60e-9	5.98	1.29e-8	5.96
	64	2.66e-13	8.08	3.02e-12	6.26	7.20e-11	6.00	2.02e-10	5.99

Table 5: Unit square, Relative eigenvalue errors, $\eta = 2k + 3$.

To assess the convergence orders, we consider a sequence of triangulations where each of the three unit squares composing the L-shaped domain Ω is discretized uniformly with $2 \times N \times N$ triangular elements, where $N = 4, 8, 16, 32, 64, 128$. Table 7 reports the relative eigenvalue errors for the first and third eigenpairs. We consider the values $\eta = 1$ and $\eta = 2k + 3$ for the stabilization parameter together with the polynomial degrees $k = 0, 1, 2$. The relative error on the first eigenvalue converges with order $h^{4/3} = h^{2t}$, whereas the relative error on the third eigenvalue converges with optimal order h^{2k+2}. These results are again in agreement with Theorem 4.4. The errors with $\eta = 2k + 3$ are, as observed above, smaller than those with $\eta = 1$. Comparing with the results reported in [32] with HDG and $k = 0$, the HHO approximation of the first eigenvalue converges with order $h^{4/3}$ whereas the HDG approximation converges with order h; the HHO approximation of the third eigenvalue converges with order h^2 whereas the HDG approximation converges with order h.

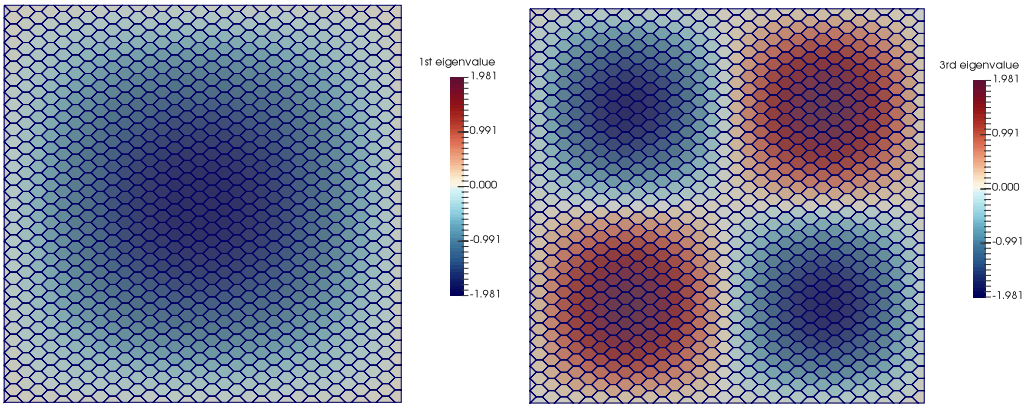

Figure 1: First and third approximate eigenfunctions with hexagonal meshes.

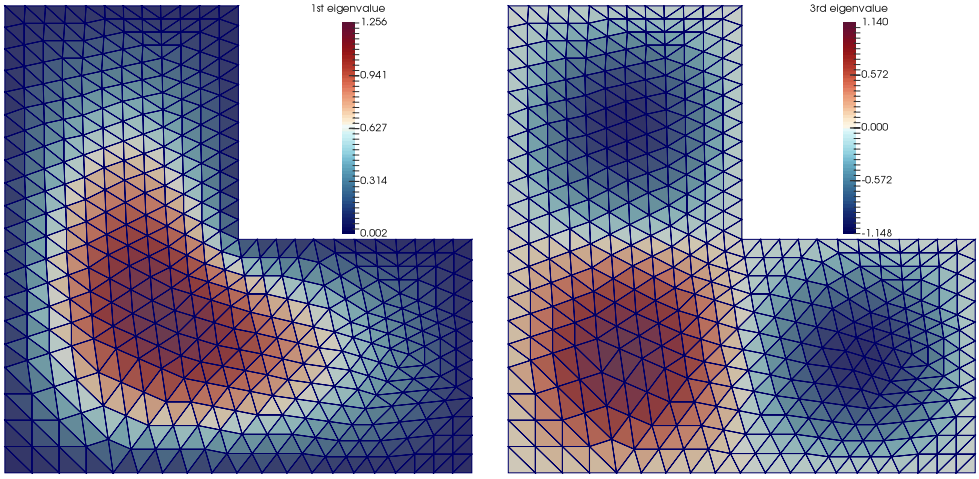

Figure 2: First and third approximate eigenfunctions in the L-shaped domain.

5.5 Unit disk

Lastly, we consider the Laplacian eigenvalue problem (2.1) in the unit disk $\Omega = \{(x, y) : x^2 + y^2 \leq 1\}$. Using polar coordinates, the eigenpairs are

$$((s_{n,m}^2, J_n(s_{n,m}r)\cos(n\theta))_{n=0,1,2,\cdots}, \qquad ((s_{n,m}^2, J_n(s_{n,m}r)\sin(n\theta))_{n=1,2,\cdots}, \tag{5.1}$$

where J_n is the Bessel function of order n, and $s_{n,m}$ are the zeros of the Bessel functions with $m = 1, 2, 3, \cdots$ Figure 3 shows the first and seventh approximate eigenfunctions.

We approximate the unit disk using a sequence of unstructured triangulations where the coarsest mesh in the sequence ($\ell = 0$) is composed of triangular cells with average diameter 0.0329182; the average diameter is halved from one mesh in the sequence to the next mesh. Since the boundary of the disk is approximated by straight lines, the error committed by this discretization is of order h^2. Thus, we only consider the lowest-order HHO approximation with $k = 0$. Table 8 reports the relative eigenvalue errors with

k	ℓ	$j=1,\eta=1$		$j=1,\eta=2k+3$		$j=3,\eta=1$		$j=3,\eta=2k+3$	
		error	order	error	order	error	order	error	order
0	0	3.20e-1	—	8.72e-2	—	6.69e-1	—	2.78e-1	—
	1	1.19e-1	1.43	2.21e-2	1.98	3.52e-1	0.93	8.41e-2	1.73
	2	3.56e-2	1.74	5.45e-3	2.02	1.28e-1	1.45	2.15e-2	1.97
	3	9.60e-3	1.89	1.35e-3	2.02	3.73e-2	1.78	5.37e-3	2.00
	4	2.48e-3	1.95	3.34e-4	2.01	9.84e-3	1.92	1.33e-3	2.01
1	0	1.97e-2	—	1.10e-3	—	3.16e-1	—	1.43e-2	—
	1	1.33e-3	3.89	8.28e-5	3.73	2.40e-2	3.72	1.32e-3	3.43
	2	8.74e-5	3.92	5.63e-6	3.88	1.45e-3	4.05	9.01e-5	3.88
	3	5.64e-6	3.95	3.66e-7	3.94	9.11e-5	3.99	5.86e-6	3.94
	4	3.59e-7	3.97	2.33e-8	3.97	5.75e-6	3.98	3.73e-7	3.97
2	0	2.99e-4	—	1.09e-5	—	4.09e-2	—	8.54e-4	—
	1	5.15e-6	5.86	2.26e-7	5.59	3.63e-4	6.82	1.42e-5	5.91
	2	8.55e-8	5.91	3.97e-9	5.83	5.59e-6	6.02	2.53e-7	5.81
	3	1.38e-9	5.95	6.52e-11	5.93	8.88e-8	5.98	4.17e-9	5.92
	4	2.21e-11	5.97	9.32e-13	6.13	1.41e-9	5.98	6.69e-11	5.96

Table 6: Unit square with hexagonal meshes, relative eigenvalue errors, $\eta = 1$ and $\eta = 2k+3$.

$\eta = 2k+3 = 3$ for the stabilization parameter. We observe a convergence order of h^2 as predicted.

6 Concluding remarks

In this paper, we devised and analyzed an approximation of the eigenvalues and eigenfunctions of a second-order elliptic operator using the Hybrid High-Order (HHO) method. Using polynomials of degree $k \geq 0$ for the face unknowns, and assuming smooth eigenfunctions, we established theoretically and observed numerically that the errors on the eigenvalues converge at rate $(2k+2)$ whereas the errors on the eigenfunctions converge at rate $(k+1)$ in the H^1-seminorm. We considered triangular and polygonal meshes in the numerical experiments for the Laplace eigenproblem in two-dimensional domains with smooth and non-smooth eigenfunctions. Additionally, we observed numerically in one dimension that the eigenvalue error converges at the even faster rate $(2k+4)$ for the particular choice $\eta = 2k+3$ of the stabilization parameter in the HHO method. Several extensions of the present work can be considered, among which we mention biharmonic eigenvalue problems and nonsymmetric second-order eigenvalue problems as well as the Maxwell eigenvalue problem in a curl-curl setting.

k	N	$j=1,\eta=1$		$j=1,\eta=2k+3$		$j=3,\eta=1$		$j=3,\eta=2k+3$	
		error	order	error	order	error	order	error	order
0	4	2.36e-1	—	1.25e-1	—	3.60e-1	—	1.82e-1	—
	8	7.79e-2	1.60	4.12e-2	1.61	1.24e-1	1.54	5.32e-2	1.77
	16	2.37e-2	1.72	1.37e-2	1.59	3.42e-2	1.86	1.39e-2	1.94
	32	7.32e-3	1.70	4.75e-3	1.53	8.77e-3	1.96	3.52e-3	1.98
	64	2.36e-3	1.63	1.71e-3	1.47	2.21e-3	1.99	8.82e-4	2.00
1	4	2.08e-2	—	1.04e-2	—	2.24e-2	—	4.62e-3	—
	8	5.92e-3	1.81	4.12e-3	1.34	1.37e-3	4.04	2.77e-4	4.06
	16	2.18e-3	1.44	1.64e-3	1.33	8.50e-5	4.01	1.72e-5	4.01
	32	8.55e-4	1.35	6.51e-4	1.33	5.31e-6	4.00	1.07e-6	4.00
	64	3.39e-4	1.34	2.58e-4	1.33	3.32e-7	4.00	6.71e-8	4.00
2	4	6.52e-3	—	4.35e-3	—	1.11e-3	—	6.08e-5	—
	8	2.48e-3	1.39	1.73e-3	1.33	1.54e-5	6.17	9.33e-7	6.03
	16	9.82e-4	1.34	6.87e-4	1.33	2.34e-7	6.04	1.44e-8	6.01
	32	3.89e-4	1.33	2.73e-4	1.33	3.63e-9	6.01	2.24e-10	6.01
	64	1.54e-4	1.33	1.08e-4	1.33	5.65e-11	6.01	3.52e-12	5.99

Table 7: L-shaped domain, relative eigenvalue errors, $\eta = 1$ and $\eta = 2k + 3$.

Acknowledgements

This publication was made possible in part by the CSIRO Professorial Chair in Computational Geoscience at Curtin University and the Deep Earth Imaging Enterprise Future Science Platforms of the Commonwealth Scientific Industrial Research Organisation, CSIRO, of Australia. Additional support was provided by the European Union's Horizon 2020 Research and Innovation Program of the Marie Skłodowska-Curie grant agreement No. 644202 and the Curtin Institute for Computation. This work was initiated when the first author was visiting the Institute Henri Poincaré (IHP) during the Fall 2016 Thematic Trimester on "Numerical Methods for Partial Differential Equations". The support of the Institute is gratefully acknowledged. Stimulating discussions with E. Burman (University College London) and J.-L. Guermond (Texas A&M University) who were also visiting the Institute for the Fall 2016 Thematic Quarter are gratefully acknowledged.

References

[1] M. Abbas, A. Ern, and N. Pignet, *Hybrid high-order methods for finite deformations of hyperelastic materials.* Available at `http://arxiv.org/abs/1709.03747`,

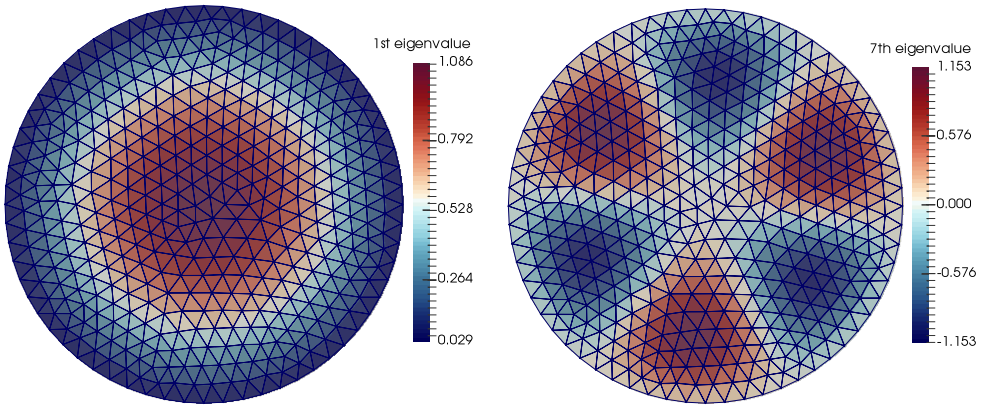

Figure 3: The first and seventh approximate eigenfunctions in the unit disk.

k	ℓ	first mode		fourth mode		seventh mode	
		error	order	error	order	error	order
	0	6.35e-3	—	1.55e-2	—	3.19e-2	—
	1	1.59e-3	2.00	3.82e-3	2.02	7.95e-3	2.00
	2	3.98e-4	2.00	9.54e-4	2.00	1.99e-3	2.00
0	3	9.96e-5	2.00	2.38e-4	2.00	4.97e-4	2.00
	4	2.49e-5	2.00	5.96e-5	2.00	1.24e-4	2.00
	5	6.22e-6	2.00	1.49e-5	2.00	3.11e-5	2.00

Table 8: Unit disk, relative eigenvalue errors, $\eta = 3$ and $k = 0$.

2017.

[2] M. Ainsworth and H. A. Wajid, *Optimally blended spectral-finite element scheme for wave propagation and nonstandard reduced integration*, SIAM J. Numer. Anal., 48 (2010), pp. 346–371.

[3] P. F. Antonietti, A. Buffa, and I. Perugia, *Discontinuous Galerkin approximation of the Laplace eigenproblem*, Comput. Methods Appl. Mech. Engrg., 195 (2006), pp. 3483–3503.

[4] D. N. Arnold, *An interior penalty finite element method with discontinuous elements*, SIAM J. Numer. Anal., 19 (1982), pp. 742–760.

[5] B. Ayuso de Dios, K. Lipnikov, and G. Manzini, *The nonconforming virtual element method*, ESAIM Math. Model. Numer. Anal., 50 (2016), pp. 879–904.

[6] I. Babuška and J. Osborn, *Eigenvalue problems*, in Handbook of Numerical Analysis, Vol. II, Handb. Numer. Anal., II, North-Holland, Amsterdam, 1991, pp. 641–787.

[7] T. Betcke and L. N. Trefethen, *Reviving the method of particular solutions*, SIAM Review, 47 (2005), pp. 469–491.

[8] D. Boffi, F. Brezzi, and L. Gastaldi, *On the problem of spurious eigenvalues in the approximation of linear elliptic problems in mixed form*, Math. Comp., 69 (2000), pp. 121–140.

[9] J. H. Bramble and J. E. Osborn, *Rate of convergence estimates for nonselfadjoint eigenvalue approximations*, Math. Comp., 27 (1973), pp. 525–549.

[10] S. C. Brenner, *Poincaré-Friedrichs inequalities for piecewise H^1 functions*, SIAM J. Numer. Anal., 41 (2003), pp. 306–324.

[11] H. Brezis, *Functional analysis, Sobolev spaces and partial differential equations*, Universitext, Springer, New York, 2011.

[12] V. Calo, Q. Deng, and V. Puzyrev, *Dispersion optimized quadratures for isogeometric analysis*, arXiv preprint arXiv:1702.04540, (2017).

[13] C. Canuto, *Eigenvalue approximations by mixed methods*, RAIRO Anal. Numér., 12 (1978), pp. 27–50.

[14] P. G. Ciarlet, *Finite Element Method for Elliptic Problems*, Society for Industrial and Applied Mathematics, Philadelphia, PA, USA, 2002.

[15] M. Cicuttin, D. A. Di Pietro, and A. Ern, *Implementation of discontinuous skeletal methods on arbitrary-dimensional, polytopal meshes using generic programming*, J. Comput. Appl. Math., (2017). To appear.

[16] B. Cockburn, D. A. Di Pietro, and A. Ern, *Bridging the Hybrid High-Order and Hybridizable Discontinuous Galerkin methods*, ESAIM: Math. Model. Numer. Anal., 50 (2016), pp. 635–650.

[17] B. Cockburn, J. Gopalakrishnan, and R. Lazarov, *Unified hybridization of discontinuous Galerkin, mixed, and continuous Galerkin methods for second order elliptic problems*, SIAM J. Numer. Anal., 47 (2009), pp. 1319–1365.

[18] B. Cockburn, J. Gopalakrishnan, F. Li, N. C. Nguyen, and J. Peraire, *Hybridization and postprocessing techniques for mixed eigenfunctions*, SIAM J. Numer. Anal., 48 (2010), pp. 857–881.

[19] Q. Deng, M. Bartoň, V. Puzyrev, and V. Calo, *Dispersion-minimizing quadrature rules for C^1 quadratic isogeometric analysis*, Comput. Methods Appl. Mech. Engrg., (2017).

[20] J. Descloux, N. Nassif, and J. Rappaz, *On spectral approximation. I. The problem of convergence*, RAIRO Anal. Numér., 12 (1978), pp. 97–112, iii.

[21] ——, *On spectral approximation. II. Error estimates for the Galerkin method*, RAIRO Anal. Numér., 12 (1978), pp. 113–119, iii.

[22] D. A. Di Pietro and J. Droniou, *A hybrid high-order method for Leray–Lions elliptic equations on general meshes*, Math. Comp., (2016).

[23] D. A. Di Pietro, J. Droniou, and A. Ern, *A discontinuous-skeletal method for advection-diffusion-reaction on general meshes*, SIAM J. Numer. Anal., 53 (2015), pp. 2135–2157.

[24] D. A. Di Pietro and A. Ern, *Discrete functional analysis tools for discontinuous Galerkin methods with application to the incompressible Navier-Stokes equations*, Math. Comp., 79 (2010), pp. 1303–1330.

[25] D. A. Di Pietro and A. Ern, *A hybrid high-order locking-free method for linear elasticity on general meshes*, Comput. Methods Appl. Mech. Engrg., 283 (2015), pp. 1–21.

[26] D. A. Di Pietro, A. Ern, and S. Lemaire, *An arbitrary-order and compact-stencil discretization of diffusion on general meshes based on local reconstruction operators.*, Comput. Meth. Appl. Math., 14 (2014), pp. 461–472.

[27] D. A. Di Pietro, A. Ern, A. Linke, and F. Schieweck, *A discontinuous skeletal method for the viscosity-dependent Stokes problem*, Comput. Methods Appl. Mech. Engrg., 306 (2016), pp. 175–195.

[28] D. A. Di Pietro and S. Lemaire, *An extension of the Crouzeix–Raviart space to general meshes with application to quasi-incompressible linear elasticity and Stokes flow*, Math. Comp., 84 (2015), pp. 1–31.

[29] R. G. Durán, L. Gastaldi, and C. Padra, *A posteriori error estimators for mixed approximations of eigenvalue problems*, Math. Models Methods Appl. Sci., 9 (1999), pp. 1165–1178.

[30] F. Gardini, *Mixed approximation of eigenvalue problems: a superconvergence result*, M2AN Math. Model. Numer. Anal., 43 (2009), pp. 853–865.

[31] S. Giani, *hp-adaptive composite discontinuous Galerkin methods for elliptic eigenvalue problems on complicated domains*, Appl. Math. Comput., 267 (2015), pp. 604–617.

[32] J. Gopalakrishnan, F. Li, N.-C. Nguyen, and J. Peraire, *Spectral approximations by the HDG method*, Math. Comp., 84 (2015), pp. 1037–1059.

[33] P. Grisvard, *Elliptic problems in nonsmooth domains*, vol. 24 of Monographs and Studies in Mathematics, Pitman (Advanced Publishing Program), Boston, MA, 1985.

[34] T. J. R. Hughes, J. A. Evans, and A. Reali, *Finite element and NURBS approximations of eigenvalue, boundary-value, and initial-value problems*, Comput. Methods Appl. Mech. Engrg., 272 (2014), pp. 290–320.

[35] F. Jochmann, *An H^s-regularity result for the gradient of solutions to elliptic equations with mixed boundary conditions*, J. Math. Anal. Appl., 238 (1999), pp. 429–450.

[36] B. Mercier, J. E. Osborn, J. Rappaz, and P.-A. Raviart, *Eigenvalue approximation by mixed and hybrid methods*, Math. Comp., 36 (1981), pp. 427–453.

[37] B. Mercier and J. Rappaz, *Eigenvalue approximation via nonconforming and hybrid finite element methods*, Publications des séminaires de mathématiques et informatique de Rennes, 1978 (1978), pp. 1–16. Available at `http://www.numdam.org/item?id=PSMIR_1978___S4_A10_0`.

[38] J. E. Osborn, *Spectral approximation for compact operators*, Math. Comp., 29 (1975), pp. 712–725.

[39] V. Puzyrev, Q. Deng, and V. Calo, *Dispersion-optimized quadrature rules for isogeometric analysis: modified inner products, their dispersion properties, and optimally blended schemes*, Comput. Methods Appl. Mech. Engrg., 320 (2017), pp. 421–443.

[40] G. Savaré, *Regularity results for elliptic equations in Lipschitz domains*, J. Func. Anal., 152 (1998), pp. 176–201.

[41] G. Strang and G. J. Fix, *An analysis of the finite element method*, vol. 212, Prentice-hall Englewood Cliffs, NJ, 1973.

[42] G. M. Vainikko, *Asymptotic error bounds for projection methods in the eigenvalue problem*, Ž. Vyčisl. Mat. i Mat. Fiz., 4 (1964), pp. 405–425.

[43] ——, *Rapidity of convergence of approximation methods in eigenvalue problems*, Ž. Vyčisl. Mat. i Mat. Fiz., 7 (1967), pp. 977–987.

[44] J. Wang and X. Ye, *A weak Galerkin finite element method for second-order elliptic problems*, J. Comput. Appl. Math., 241 (2013), pp. 103–115.